IN THE UNITED STATES PATENT AND TRADEMARK OFFICE

In re application of: Zagoskin	)	Art Unit: 2814
	)	Examiner: Douglas A. Wille
Serial No. 09/452,749 Filed: December 1, 1999	)	Attorney Docket: 11090-003-999
For: Permanent Readout Superconducting Qubit	)	

DECLARATION OF DR. ALEXANDER TZALENCHUK UNDER 37 C.F.R. § 1.132

Assistant Commissioner for Patents
Washington, D.C. 20231

Sir:

I, ALEXANDER TZALENCHUK, declare and state as follows:

1. I am a citizen of Russia currently residing at 244 Ashburnham Road, Ham / Richmond, Surrey, United Kingdom TW10 7SA.

2. I am familiar with the specification and claims of the above-identified patent application ("Application"), the Office Action mailed February 19, 2003, United States Patent 5,157,466 to Char *et al.* (hereinafter "Char *et al.*") and Tinkham, *Introduction to Superconductivity*, Second Edition, (hereinafter "Tinkham").

3. I am an employee of the National Physics Laboratory of the United Kingdom of Great Britain and Northern Ireland and its affiliate NPL Management Limited (herein after "NPL"). NPL is located in Teddington, Middlesex, UK, TW11 0LW, where I am employed by it as a Senior Research Scientist in its Fundamental and Wavelength Standards Team. NPL has entered into a collaborative research agreement with D-Wave Systems Inc.

(hereinafter "D-Wave"), the assignee herein, dated March 27, 2002, whereby NPL carries out certain research and measurement work for D-Wave. One product of this research and measurement work is the creation of certain intellectual property, including patent applications, all rights, title and interest to which are held by D-Wave pursuant to the terms and conditions of the aforementioned collaborative research agreement.

4. I received a B.A. in Electronics Engineering from the Chair of Crystal Physics, Faculty of Electronic Materials and Devices, Moscow Steel and Alloys Institute and a Ph.D. in Physics and Mathematics from the A.V. Shubnikov Institute of Crystallography Russian Academy of Sciences, and have been actively performing research in the field of solid state and superconducting fabrication and characterization for the past nineteen years. During that time, I have published in excess of 35 articles in the fields of solid state physics, superconducting structure fabrication, and characterization of superconducting structures and have six allowed or issued patents. My research experience encompasses work in semi conductor structures formed on bi-crystal substrates, bi-crystal substrates for high-Tc superconductors, mesoscopic effects in high-Tc superconductors, Josephson phenomena in high-Tc bi-crystals and bi-epitaxial grain boundary Josephson junctions, and Josephson phenomena in high-Tc step edge Josephson junctions, and qubits using high-Tc Josephson junctions. I am a specialist in the fabrication of microstructures in high-Tc superconducting devices, these include three terminal devices, SQUIDs, and qubits. I have additional expertise in the characterization of superconducting devices including instrumentation for scanning SQUID/Hall microscopy, and investigation of local magnetization and superconductivity. I have received an individual George Soros Foundation grant, on the basis of high citation index, and the Swedish Foundation for International Cooperation in Research and Higher Education, through a program to bring eminent foreign scientists and scholars to Sweden.

5. I declare that a clean Josephson junction formed using a d-wave superconducting material is defined by a current-phase relationship in which the second harmonic makes a distinct contribution to the current-phase relationship of the clean Josephson junction.

6. I declare that the second harmonic effect on the current-phase relationship of a clean Josephson junction formed using a d-wave superconducting material is temperature dependent.

7. I declare that, in the current state of the art, the second harmonic effect on the current-phase relationship of clean Josephson junctions formed using d-wave superconducting material cannot be precisely engineered.

8. I declare that, because of the temperature dependence of the second harmonic effect and the inability to precisely engineer the second harmonic effect, it would be undesirable to form a dc SQUID using clean Josephson junctions in a d-wave superconducting material, such as $YBa_2Cu_3O_{7-x}$ (YBCO), when the dc SQUID is intended for use in commercial SQUID magnetometers such as those described in Char *et al.*

9. I declare that Chapter 7 of Tinkham only considers conventional superconducting materials and devices made out of conventional superconducting materials.

10. I declare that, based on my experience in the field of bi-epitaxial technology, neither the bi-epitaxial technology described in Char et al. nor the best quality crystal structures available for bi-epitaxial Josephson junction technology were sufficiently advanced at the time of filing of the Application to prepare a clean Josephson junction such as that

described in the Application.

11. I further declare, under penalty of perjury under the laws of the United States of America, that all statements made herein of my own knowledge are true and that these statements were made with the knowledge that willful false statements and the like are

punishable by fine or imprisonment, or both, under Section 1001 or Title 18 of the United States Code.

Date: 16/04/03

Dr. Alexander Tzalenchuk

Anomalous periodicity of the current-phase relationship of grain-boundary Josephson junctions in high-T_c superconductors

E. Il'ichev, V. Zakosarenko, R. P. J. IJsselsteijn, H. E. Hoenig, V. Schultze, and H.-G. Meyer
Department of Cryoelectronics, Institute for Physical High Technology, P.O. Box 100239, D-07702 Jena, Germany

M. Grajcar and R. Hlubina
Department of Solid State Physics, Comenius University, Mlynská Dolina F2, 842 15 Bratislava, Slovakia
(Received 28 January 1999)

The current-phase relation (CPR) for asymmetric 45° Josephson junctions between two *d*-wave superconductors has been predicted to exhibit an anomalous periodicity. We have used the single-junction interferometer to investigate the CPR for these kinds of junctions in $YBa_2Cu_3O_{7-x}$ thin films. A remarkable amplitude of the π-periodical component of the CPR has been experimentally found, providing an additional source of evidence for the *d*-wave symmetry of the pairing state of the cuprates. [S0163-1829(99)05629-5]

A number of experimental results confirm $d_{x^2-y^2}$-wave symmetry of the pairing state of high-temperature superconductors.[1] An unconventional pairing state requires the existence of zeros of the order parameter in certain directions in momentum space. Thermodynamic and spectroscopic measurements do indeed suggest their existence, but by themselves they do not exclude conventional *s*-wave pairing with nodes.[1] Direct evidence for the *d*-wave pairing state is provided by phase-sensitive experiments, which are based on the Josephson effect.[2] Quite generally, the current-phase relationship (CPR) of a Josephson junction, $I(\varphi)$ is an odd periodic function of φ with a period 2π.[3]. Therefore $I(\varphi)$ can be expanded in a Fourier series

$$I(\varphi)=I_1\sin\varphi+I_2\sin 2\varphi+\cdots. \tag{1}$$

In the tunnel limit we can restrict ourselves to the first two terms in Eq. (1). Since the order parameter is bound to the crystal lattice, $I(\varphi)$ of a weak link depends on the orientation of the *d*-wave electrodes with respect to their boundary. The existing phase-sensitive experiments exploit possible sign changes of I_1 between different geometries.[2] In this work we present a phase-sensitive experimental test of the pairing state symmetry of cuprates. Namely, in certain geometries, the I_1 term should vanish by symmetry. In such cases, the CPR should exhibit an anomalous periodicity.

Let us analyze the angular dependence of $I_{1,2}$ in a junction between two macroscopically tetragonal *d*-wave superconductors. As emphasized in Ref. 4, also heavily twinned orthorhombic materials such as $YBa_2Cu_3O_{7-x}$ belong to this class, if the twin boundaries have odd symmetry. We consider an ideally flat interface between two superconducting electrodes. Let θ_1 (θ_2) denote the angle between the normal to the grain boundary and the *a* axis in electrode 1 (2), see Fig. 1. If we only keep the lowest-order angular harmonics, the symmetry of the problem dictates that[4]

$$I_1=I_c\cos 2\theta_1\cos 2\theta_2+I_s\sin 2\theta_1\sin 2\theta_2. \tag{2}$$

The coefficients I_c, I_s are functions of the barrier strength, temperature T, etc. The I_2 term results from higher-order tunneling processes and we neglect its weak angular dependence. It is seen from Eq. (2) that the criterion for the observation of an anomalous period of the CPR, $I_1=0$, is realized for an asymmetric 45° junction, i.e., a junction with $\theta_1=45°$ and $\theta_2=0$.

The I_2 term is also present in weak links based on conventional *s*-wave superconductors but for all known types of weak links $|I_2/I_1|<1$. For instance, for a tunnel junction $|I_2/I_1|\ll 1$. For a superconductor–normal-metal–superconductor (SNS) junction, $I\propto\sin\varphi/2$ at $T=0$,[5] and the Fourier expansion of Eq. (1) leads to $I_2/I_1=-2/5$. Therefore a possible experimental observation of $|I_2/I_1|\gg 1$ in an asymmetric 45° junction provides direct evidence of *d*-wave symmetry of the pairing state in the cuprates.

We have investigated the CPR of $YBa_2Cu_3O_{7-x}$ thin-film bicrystals with asymmetric 45° [001]-tilt grain boundaries as sketched in Fig. 1, using a single-junction interferometer configuration in which the Josephson junction is inserted into a superconducting loop with a small inductance L. In a stationary state without fluctuations, the phase difference φ across the junction is controlled by applying an external magnetic flux Φ_e penetrating the loop: $\varphi=\varphi_e-\beta f(\varphi)$. Here $\varphi_e=2\pi\Phi_e/\Phi_0$; $\Phi_0=2.07\times10^{-15}$ Tm^2 is the flux quantum; $f(\varphi)=I(\varphi)/I_0$ is the CPR normalized to the maximal Josephson current I_0, and $\beta=2\pi LI_0/\Phi_0$ is the normalized

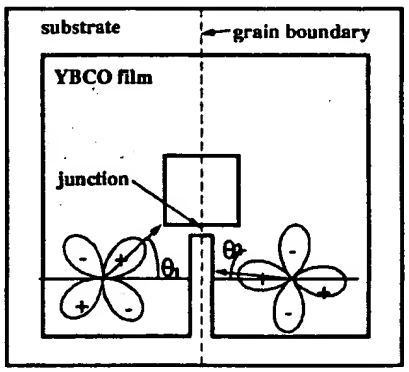

FIG. 1. Washer-shaped interferometer with one short Josephson junction (not in scale). Dimensions are given in the text.

critical current. In order to obtain the CPR for the complete phase range $-\pi \leq \varphi \leq \pi$ the condition $\beta < 1$ has to be fulfilled, because for $\beta > 1$ the curve $\varphi(\varphi_e)$ becomes multivalued. Following Ref. 3, we express the effective inductance of the interferometer using the derivative f' with respect to φ as $L_{int} = L[1 + 1/\beta f'(\varphi)]$. The inductance can be probed by coupling the interferometer to a tank circuit with inductance L_T, quality factor Q, and resonance frequency ω_0 through the mutual inductance M.[8] External flux in the interferometer is produced by a current $I_{dc} + I_{rf}$ in the tank coil and can be expressed as $\varphi_e = 2\pi(I_{dc} + I_{rf})M/\Phi_0 = \varphi_{dc} + \varphi_{rf}$, where $M^2 = k^2 L L_T$ with k a coupling coefficient. Taking into account the quasiparticle current in the presence of a voltage V across the junction the phase difference is given by the relation $\varphi = \varphi_{dc} + \varphi_{rf} - \beta f(\varphi) - 2\pi\tau(\varphi)V/\Phi_0$, where $\tau(\varphi) = L/R_J(\varphi)$ with $R_J(\varphi)$ the resistance of the junction. In the small-signal limit $\varphi_{rf} \ll 1$ and in the adiabatic case $\omega\tau \ll 1$, keeping only the first-order terms, the effective inductance L_{eff} of the tank circuit-interferometer system is

$$L_{eff} = L_T\left(1 - k^2 \frac{L}{L_{int}}\right) = L_T\left(1 - \frac{k^2 \beta f'(\varphi)}{1 + \beta f'(\varphi)}\right).$$

Thus the phase angle α between the driving current and the tank voltage U at the resonance frequency of the tank circuit ω_0 is

$$\tan\alpha(\varphi) = \frac{k^2 Q \beta f'(\varphi)}{1 + \beta f'(\varphi)}. \tag{3}$$

Using the relation $[1 + \beta f'(\varphi)]d\varphi = d\varphi_{dc}$ which is valid for $\varphi_{rf} \ll 1$ and $\omega\tau \ll 1$, one can find the CPR from Eq. (3) by numerical integration.

The advantage of the CPR measurement of an asymmetric 45° junction with respect to the by-now standard phase-sensitive tests of pairing symmetry based on the angular dependence of I_1 is twofold. First, it avoids the complications of the analysis of experiments caused by the presence of the term I_s.[4] Second, flux trapped in the interferometer washer (see Fig. 1) does not invalidate the conclusions about the ratio $|I_2/I_1|$ and hence about the pairing symmetry, which is not the case in standard phase-sensitive tests of the d-wave symmetry of the pairing state.[9]

The films of 100-nm thickness were fabricated using standard pulsed laser deposition on (001) oriented $SrTiO_3$ bicrystalline substrates with asymmetric [001] tilt misorientation angles of 45°±1°. The films were subsequently patterned by Ar ion-beam etching into 4×4-mm^2 square washer single-junction interferometer structures (Fig. 1). The widths of the junctions were 1–2 μm. The square washer holes had a side length of 50 μm. This geometry of the interferometer gives $L \approx 80$ pH. The resistance of a similar single junction (without interferometer loop) was measured directly and $R_J > 1$ Ω was found. Therefore the condition for the adiabatic limit $\omega\tau \ll 1$ is satisfied. For measurements of $\alpha(\varphi_{dc})$, several tank circuits with inductances 0.2–0.8 μH and resonance frequencies 16–35 MHz have been used. The unloaded quality factor of the tank circuits $70 < Q < 150$ has been measured at various temperatures. The coupling factor k was determined from the period ΔI_{dc} of $\alpha(I_{dc})$ using $M\Delta I_{dc} = \Phi_0$. Its value varied between 0.03 and 0.09. The amplitude of I_{rf} was set to produce a flux in the interferometer smaller than 0.1 Φ_0 to ensure the small-signal limit.

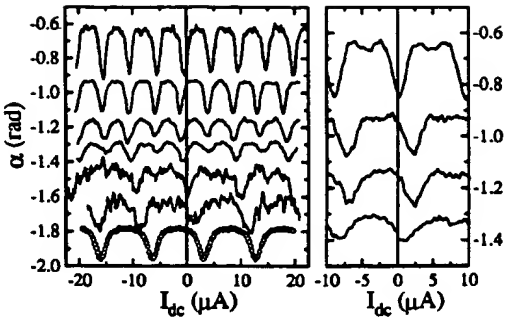

FIG. 2. Left panel: Phase angle between the driving current and the output voltage measured for sample No. 1 at different temperatures as a function of the dc current I_{dc}. The curves are shifted along the y axis and the data for $T = 30$ and 40 K are multiplied by factor 4 for clarity. From top to bottom, the data correspond to $T = 4.2$, 10, 15, 20, 30, and 40 K. The data measured for 36° bicrystals ($\theta_1 \approx 36°, \theta_2 \approx 0$) at $T = 40$ K in the same washer geometry are shown for comparison (open circles). Right panel: The same for sample No. 3. From top to bottom, the data correspond to $T = 4.2$, 10, 15, and 20 K.

The measurements have been performed in a gas-flow cryostat with a five-layer magnetic shielding in the temperature range $4.2 \leq T < 90$ K. The experimental setup was calibrated by measuring interferometers of the same size with 24° and 36° grain boundaries. We have studied six samples, out of which for four samples the π-periodic component of $I(\varphi)$ was experimentally observed. At low temperatures for two samples (Nos. 1 and 2) the value of I_2 is larger than I_1. For sample Nos. 3 and 4 I_2 is approximately 10–20 % of I_1 and for sample Nos. 5 and 6 I_2 is negligible. As an example we plot the phase angle α as a function of the dc current I_{dc} for sample Nos. 1 and 3 (Fig. 2). The behavior of sample No. 1 at low temperatures is defined by the π periodic component of $I(\varphi)$. The curves for sample No. 3 are 2π-periodic, nevertheless for the curve at $T = 4.2$ K the local minima clearly show the presence of a π-periodic component.

In order to determine the CPR we assume that the period of $\alpha(I_{dc})$ at $T = 40$ K and $\Delta I_{dc} = 9.6$ μA, corresponds to $\Delta\varphi_{dc} = 2\pi$. We take $\varphi_{dc} = 0$ at a maximum or minimum of α. This is necessary in order to satisfy $I(\varphi = 0) = 0$, as required by general principles.[3] The experimentally observed shift of the first extreme of $\alpha(I_{dc})$ from $I_{dc} = 0$ (Fig. 2) can be due to flux trapped in the interferometer washer. Most probably, this flux resides in the long junction originated by the grain boundary crossing the washer of the interferometer. This long junction does not play an active role because the Josephson penetration depth is much smaller than the junction length, and external fields produced by I_{dc} are smaller than the first critical field. Nevertheless, the long junction sets the phase difference for $I_{dc} = 0$ at the small junction.

In Fig. 3, we show the CPR determined from the data in Fig. 2. For all curves we have performed a minimal necessary shift consistent with $I(\varphi = 0) = 0$. Thus we have assumed that at $\varphi_{dc} = 0$ a minimum of $\alpha(\varphi_{dc})$ is realized. For an interferometer with a conventional s-wave weak link (and also for the 36° junction), at $\varphi_{dc} = 0$ one gets a maximum of

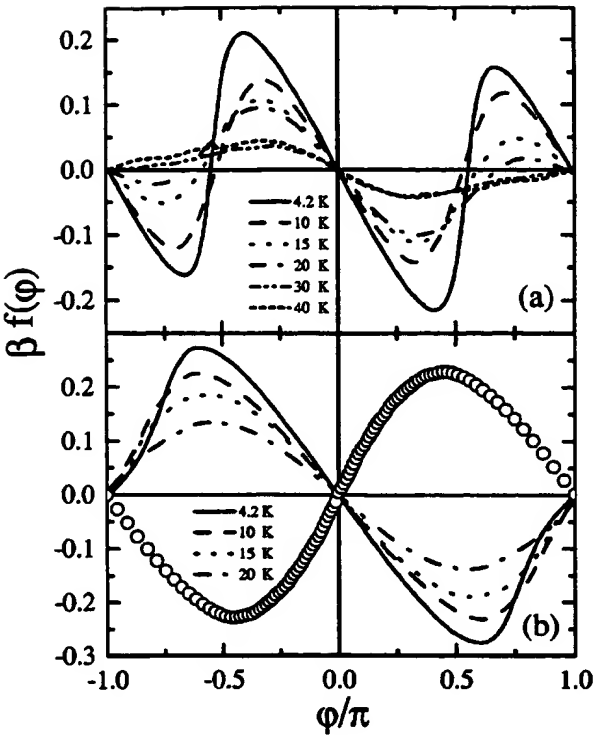

FIG. 3. (a) Josephson current through the junction for sample No. 1 as a function of the phase difference φ, determined from the data in Fig. 2. The scattering of $\alpha(\varphi)$ values was reduced by folding the data back to the interval $\langle 0,\pi\rangle$ and taking the average. Here, the symmetry $\alpha(\varphi)=\alpha(-\varphi)$ was assumed. (b) The same for sample No. 3. The data for the asymmetric 36° bicrystal at $T=40$ K (open circles) are also shown.

$\alpha(\varphi_{dc})$. Note that the minimum of $\alpha(\varphi_{dc})$ at $\varphi_{dc}=0$ implies a paramagnetic response of the interferometer in the limit of small applied fields.

The amplitude of the π-periodic component of the CPR decreases drastically with increasing temperature, and at $T=40$ K its contribution is negligible for all samples. The temperature dependence of I_1 and I_2 could be determinated with acceptable accuracy for sample No. 1 only. With decreasing T, $|I_2|$ grows monotonically down to $T=4.2$ K, while the I_1 component exhibits only a weak temperature dependence (Fig. 4).

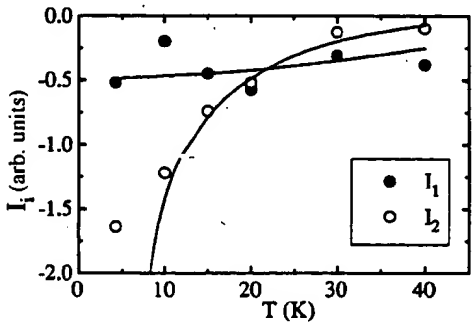

FIG. 4. Temperature dependence of the Fourier expansion coefficients $I_{1,2}$ determined from the experimental data in Fig. 3(a). Solid lines are the Fourier expansion coefficients for the numerical data in Fig. 5.

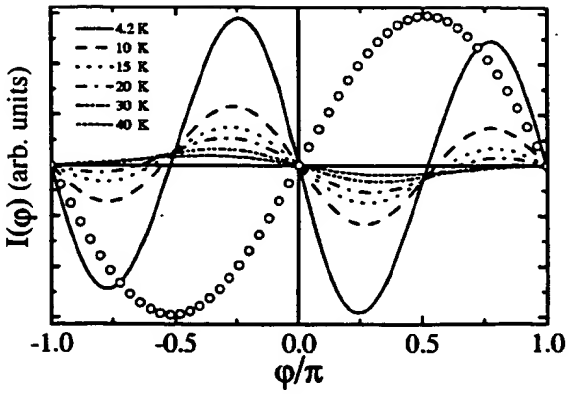

FIG. 5. $I(\varphi)$ calculated according to Eq. (64) of Ref. 11 for a junction with $\theta_1=45.5°$, $\theta_2=0$, $\lambda d=1.5$, $\kappa=0.5$, and $T_c=60$ K. $I(\varphi)$ at $T=40$ K for the 36° bicrystal (open circles) was calculated with the same parameters except for $\theta_1=36°$.

Our experimental results can be understood as follows. It is well known that the microstructural properties of the grain boundaries, especialy 45° boundaries, are defined by their faceted nature. Faceting is an intrinsic property of the grain boundaries,[6,7] and, due to d-wave symmetry of the order parameter, the properties of the junctions strongly depend on the particular distribution of the facets. Small deviations from the ideal geometry of the asymmetric 45° junction lead to a finite value of I_1. Thus for nearly ideal junctions $|I_2/I_1|\gg 1$ at $T\to 0$. The region $T\sim T_c$ can be analyzed quite generally within the Ginzburg-Landau theory. Let the electrodes be described by the (macroscopic) order parameters $\Delta_{1,2}=|\Delta|e^{i\varphi_{1,2}}$. Then the phase-dependent part of the energy of the junction is $E=a[\Delta_1\Delta_2^*+\text{H.c.}]+b[(\Delta_1\Delta_2^*)^2+\text{H.c.}]+\cdots$ where $a,b,\ldots$ depend weakly on T.[10] Thus for T close to T_c we estimate $I_1\propto|\Delta|^2\propto(T_c-T)$ and $I_2\propto|\Delta|^4\propto(T_c-T)^2$, leading to $|I_2/I_1|\ll 1$. With increasing deviations from ideal geometry $|I_2/I_1|$ decreases. For large enough deviations, negligible values of $|I_2|$ are expected. These expectations are qualitatively consistent with the experimental data (see also Fig. 4).

So far, our discussion was based solely on symmetry arguments. Let us attempt a more quantitative analysis of our data now. Two different microscopic pictures of asymmetric 45° Josephson junctions between d-wave superconductors have been considered in the literature. The first picture assumes a microscopically tetragonal material and an ideally flat interface.[10-12] Within this picture, only sample No. 1 can be analyzed. Sample No. 2 had $I_0(T=1.5\ \text{K})\cong 10^{-2}\mu$A. At this temperature only the π-periodic component of $I(\varphi)$ was observed. At higher temperatures I_0 was not measurable. $I(\varphi)$ for sample No. 1 calculated according to the model of Ref. 11 is shown in Fig. 5. The experimental data can be fitted within a relatively broad range of barrier heights. However, if we require the $I(\varphi)$ relation of the 36° junction to be fitted by the same (or smaller) barrier height as for the 45° junction, we conclude the barrier of the 45° junction to be rather low.[14] The dependence of $I(\varphi)$ on T requires a choice of $T_c\approx 60$ K in the non-self-consistent theory of Ref. 11. The reduction from the bulk $T_c=90$ K is probably due to a combined effect of surface degradation and order-parameter suppression at the sample surface. The temperature dependence

of the ratio of the π and 2π periodic components in $I(\varphi)$ is seen to be in qualitative agreement with experimental data in Fig. 3(a). This is explicitly demonstrated in Fig. 4 where we compare the experimentally obtained $I_{1,2}$ with the results of the Fourier analysis of the curves in Fig. 5. The divergence of I_2 as $T \to 0$ is an artifact of the ideal junction geometry assumed in Ref. 11. If a finite roughness of the interface is taken into account, this divergence is cut off and the experimental data in Fig. 4 do indeed resemble theoretical predictions for a rough interface.[12] However, the non-self-consistent theory of Ref. 11 is unable to explain the experimentally observed steep CPR close to the minima of the junction energy [see Fig. 3(a)].

In a different approach a heavily meandering interface with $\theta_i = \theta_i(x)$ is assumed. Now, the critical current density $j_c(x)$ is a random function with a typical amplitude $\langle |j_c(x)| \rangle \sim j_c$. If the average critical current along the junction $\langle j_c \rangle < j_c$, a remarkable π-periodic component is present in the CPR. The relation $|I_2/I_1|$ depends on the distribution of $j_c(x)$ and can be much larger than one for $\langle j_c \rangle \ll j_c$.[15,16] This model qualitative explains the obtained results for all samples, however for a quantitative comparison the actual microscopic distribution $j_c(x)$ should be known. Note that also within the picture of Refs. 15 and 16 the d-wave symmetry of the pairing state is crucial, otherwise the condition $\langle j_c \rangle \ll j_c$ is difficult to satisfy.

Our present understanding of $I(\varphi)$ in the asymmetric 45° junction is only qualitative. We cannot say whether the remarkable amplitude of the π-periodic component of $I(\varphi)$ is dominated by the microscopically flat regions,[13] or due to the spatial inhomogeneity of the junction. This issue requires further study.

In conclusion, we have measured the magnetic-field response of a single-junction interferometer based on asymmetric 45° grain-boundary junctions in $YBa_2Cu_3O_{7-x}$ thin films. A large π-periodic component of $I(\varphi)$ has been experimentally found, which is in agreement with theoretical predictions for $d_{x^2-y^2}$-wave superconductors. Hence our results provide an additional source of evidence for the d-wave symmetry of the pairing state in the cuprates.

Financial support by the DFG (Ho 461/3-1) and partial support by INTAS (N 11459) are gratefully acknowledged. M. G. and R. H. were supported by the Slovak Grant Agency (Grant No. 1/4300/97) and the Comenius University (Grant No. UK/3927/98).

[1] For a review, see J. Annett, N. Goldenfeld, and A. J. Leggett, in *Physical Properties of High Temperature Superconductors*, edited by D. M. Ginsberg (World Scientific, New Jersey, 1996), Vol. V.

[2] See C. C. Tsuei *et al.*, Science **271**, 329 (1996), and references therein.

[3] A. Barone and G. Paterno, *Physics and Applications of the Josephson Effect* (Wiley, New York, 1982).

[4] M. B. Walker and J. Luettmer-Strathmann, Phys. Rev. B **54**, 588 (1996).

[5] I. O. Kulik and A. N. Omel'yanchuk, Fiz. Nizk. Temp. **4**, 296 (1978) [Sov. J. Low Temp. Phys. **4**, 142 (1978)].

[6] H. Hilgenkamp, J. Mannhart, and B. Mayer, Phys. Rev. B **53**, 14 586 (1996).

[7] J. Mannhart *et al.*, Phys. Rev. Lett. **77**, 2782 (1996).

[8] E. V. Il'ichev *et al.*, J. Low Temp. Phys. **106**, 503 (1997).

[9] R. A. Klemm, Phys. Rev. Lett. **73**, 1871 (1994).

[10] A. Huck, A. van Otterlo, and M. Sigrist, Phys. Rev. B **56**, 14 163 (1997).

[11] Y. Tanaka and S. Kashiwaya, Phys. Rev. B **56**, 892 (1997).

[12] Y. S. Barash, H. Burkhardt, and D. Rainer, Phys. Rev. Lett. **77**, 4070 (1996).

[13] C. R. Hu, Phys. Rev. Lett. **72**, 1526 (1994).

[14] This is consistent with the Fourier analysis of the data in Fig. 3 which results in a non-negligible I_n also for $n \geq 3$.

[15] A. J. Millis, Phys. Rev. B **49**, 15 408 (1994).

[16] R. G. Mints, Phys. Rev. B **57**, R3221 (1998).

Nonsinusoidal Current-Phase Relationship of Grain-Boundary Josephson Junctions in High-T_c Superconductors

E. Il'ichev, V. Zakosarenko, R. P. J. IJsselsteijn, V. Schultze, H.-G. Meyer, and H. E. Hoenig
Department of Cryoelectronics, Institute for Physical High Technology, P.O. Box 100239, D-07702 Jena, Germany

H. Hilgenkamp and J. Mannhart
Experimental Physics VI, Center for Electronic Correlations and Magnetism, Institute of Physics, Augsburg University, D-86135 Augsburg, Germany
(Received 13 January 1998)

For various configurations of Josephson junctions incorporating superconductors with unconventional order parameter symmetry, such as most high-T_c cuprates, deviations from the standard sinusoidal current-phase dependence have been predicted. To this point, these deviations have never been observed experimentally. We have measured the current-phase relation of high-T_c Josephson junctions, namely, $YBa_2Cu_3O_{7-x}$ thin film bicrystals, comprising symmetric 45° [001] tilt grain boundaries. The current-phase relations of all junctions investigated were found to be extremely nonharmonic, in agreement with a $d_{x^2-y^2}$-wave dominated symmetry of the order parameter. [S0031-9007(98)06674-5]

PACS numbers: 74.50.+r

The current-phase relation (CPR) $f(\varphi)$ is a characteristic property of any weak link connecting two superconductors. It describes the dependence of the Cooper-pair current I_p on the phase difference φ of the order parameters of both superconducting electrodes. In a general form it is expressed as

$$I_p = I_c f(\varphi), \qquad -1 \le f(\varphi) \le 1, \tag{1}$$

I_c being the critical current of the weak link. It was shown by Josephson [1] that for ideal tunnel junctions between conventional superconductors the CPR is sinusoidal, i.e., $f(\varphi) = \sin(\varphi)$. This sinusoidal dependence has been confirmed experimentally numerous times for standard tunnel junctions between conventional superconductors [2].

Recently, it has been revealed that the order parameter of most high-T_c cuprates is unconventional, dominated by a $d_{x^2-y^2}$ symmetry component [3–5]. Because of the sign change of the order parameter associated with this symmetry, strong deviations from the standard sinusoidal dependence have been predicted for the current-phase relations of various configurations of Josephson junctions employing such unconventional superconductors [6–9]. In particular, nonharmonic and double-periodic current-phase relations are expected for junctions oriented nominally perpendicular to the ⟨110⟩ direction of one or of both electrodes, as well as for junctions for which the ⟨110⟩ direction of one of the electrodes is aligned with the ⟨100⟩ direction of the other, such as for 45° [001] tilt grain boundaries.

These predictions are highly unusual. Therefore, an experimental clarification of the CPR for high-T_c junctions for which deviations from a standard harmonic behavior are expected is desirable. Such experiments will further enhance the understanding of the influence of the order parameter symmetry on the properties of grain boundaries and high-T_c Josephson junctions. In addition, they will provide valuable information for the design and use of Josephson junction-based circuits, of which many characteristics directly depend on the CPR. However, to our knowledge, such experiments have not been carried out. All available data refer to Josephson junctions for which nominally sinusoidal current-phase relations are expected. The CPR was measured for weak links prepared by ion irradiation [10], for step-edge junctions [11,12], and also for 24° bicrystal grain boundaries [12]. In nearly all of these cases sinusoidal current-phase relations were found. Deviations from a sinusoidal dependence have been observed only for one step-edge junction, measured at 77 K [12]. These deviations can be explained by the influence of thermal noise [13].

For these reasons we have investigated the CPR of $YBa_2Cu_3O_{7-x}$ thin film bicrystals with symmetric 45° [001]-tilt grain boundaries, as sketched in Fig. 1(a). For these junctions, strong deviations from a sinusoidal CPR are anticipated.

Following a standard approach [14], the CPR was measured using a single-junction interferometer configuration in which the Josephson junction is part of a superconducting loop with a small inductance L. The phase difference φ across the junction is controlled by applying an external magnetic flux Φ_e penetrating the loop:

$$\varphi = \varphi_e - \beta f(\varphi) + \varphi_n + 2\pi m. \tag{2}$$

Here, $\varphi_e = 2\pi\Phi_e/\Phi_0$ is the external flux normalized to the flux quantum Φ_0 ($= 2.07 \times 10^{-15}$ Tm^2). The constant $\beta = 2\pi L I_c/\Phi_0$ is the normalized critical current, φ_n is a term accounting for the effective noise, and m is

 0031-9007/98/81(4)/894(4)$15.00

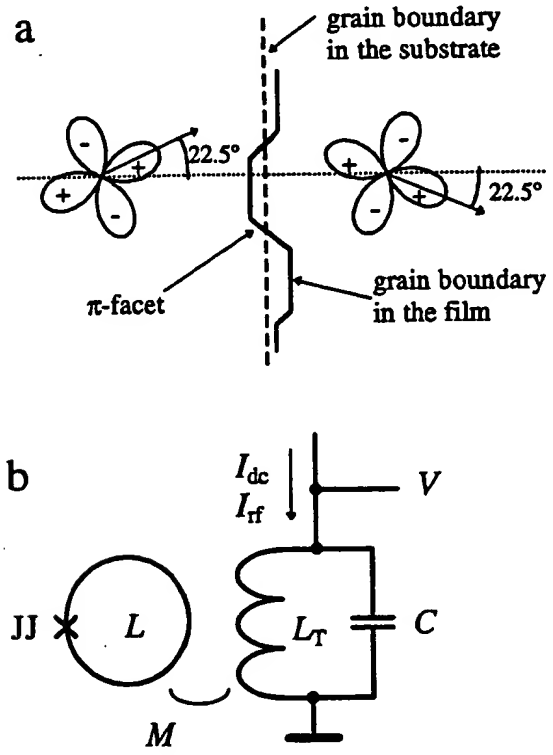

FIG. 1. (a) Schematic representation of a symmetric 45° [001]-tilt grain boundary junction in a $d_{x^2-y^2}$ superconductor. The boundary in the superconducting thin film is meandering, leading to the occurrence of π facets. (b) Schematic of the measurement setup. The Josephson junction is denoted by JJ, and C indicates the capacitance of the tank circuit. The other denotations are explained in the text.

an integer. As capacitive contributions to the loop current are insignificant at the measurement frequencies, the junction capacitance has been neglected. The quasiparticle current is also negligible, for reasons discussed below.

The superconducting loop is inductively coupled to a tank circuit with inductance L_T [see Fig. 1(b)]. This tank circuit is driven with a current I_{rf} at a frequency ω and a dc current I_{dc}. Thus, φ_e can be expressed as a sum of a dc and an rf component $\varphi_e = \varphi_{dc} + \varphi_{rf}$. In this arrangement, the effective impedance $Z_{eff}(\omega)$ of the loop-tank circuit combination is a function of φ_e. As shown by Rifkin and Deaver [14], the CPR can be obtained from this dependence, provided that $\varphi_{rf} \ll 1$. To obtain the CPR for the complete phase range $0 \le \varphi \le 2\pi$, the condition $\beta < 1$ has to be fulfilled in addition.

To enhance the accuracy of the measurement, we have adapted this common approach and retrieved the CPR from a measurement of the φ_{dc} dependence of the phase angle α between the drive current I_{rf} and the tank voltage V at the resonant frequency of the tank circuit ω_0. As described in Ref. [12], at ω_0, the $\alpha(\varphi_{dc})$ dependence is related to the derivative of the CPR $f'(\varphi) \equiv df(\varphi)/d\varphi$ in the following way:

$$\tan\alpha(\varphi_{dc}) = \frac{k^2 Q \beta f'(\varphi(\varphi_{dc}))}{1 + \beta f'(\varphi(\varphi_{dc}))}. \quad (3)$$

Here k is the coupling factor between the tank inductance and the interferometer, $k^2 = M^2/(LL_T)$, where M is the mutual inductance [Fig. 1(b)]. Using Eq. (3), from the measured $\alpha(\varphi_{dc})$ dependence $f'(\varphi(\varphi_{dc}))$ is obtained. The CPR is restored by integrating $f'(\varphi(\varphi_{dc}))$ numerically, using the $d\varphi(\varphi_{dc})/d\varphi_{dc}$ dependence obtained from differentiating Eq. (2) with respect to φ_{dc}.

The samples investigated consisted of three bicrystalline $YBa_2Cu_3O_{7-x}$ films with a T_c ($R = 0$) of 88 K. The films, with thickness $t = 100$ nm, were deposited by standard pulsed laser deposition on (001)-oriented $SrTiO_3$ bicrystalline substrates [15] with symmetric [001]-tilt misorientation angles of 45° ± 2° and were subsequently patterned by Ar ion-beam etching into 8×8 mm^2 or 5×5 mm^2 square washer single-junction interferometer structures. The widths of the junctions were $b \approx 2$–3 μm. The washer holes had a side length of 50 μm, leading to $L \approx 80$ pH.

To minimize the influence of external noise, the samples were measured in superconducting and double magnetic shielding at a temperature of 4.2 K. The condition $\beta < 1$ for the investigated interferometers was confirmed experimentally from the character of its response versus φ_{dc} [12].

$YBa_2Cu_3O_{7-x}$ grain boundaries with a symmetric [001] tilt angle of 45° typically have a normal-state interface-resistivity $\rho_n > 1 \times 10^{-8}$ Ω cm^2, which we also measured for boundaries fabricated under identical conditions as the junctions used in the present experiments. In the configuration used, this ρ_n corresponds to normal-state resistances $R_n > 1$ Ω. Accordingly, the relaxation time of the interferometer $\tau = L/R$ is short ($\tau \ll 1/\omega_0$), and hence the quasiparticle current is negligible [12].

For the measurements of $\alpha(\varphi_{dc})$, two tank circuits with quality factor $Q = 120$ and inductance $L_T = 0.4$ μH, $\omega_0 = 30$ MHz, and $L_T = 0.73$ μH, $\omega_0 = 23$ MHz, respectively, were employed. The phase angle was recorded as a function of I_{dc} after amplification of the tank voltage by a high-impedance amplifier. The coupling coefficient k was determined from the period of the $\alpha(I_{dc})$ dependence. Values of $k = 0.072$ and $k = 0.054$ for the respective tank circuits are obtained. To ensure the validity of the small-signal limit, the measurements were carried out with $\varphi_{rf} < 0.15$.

A typical $\alpha(I_{dc})$ dependence is shown in Fig. 2. The corresponding CPR, depicted in Fig. 3, is clearly deviating from the standard sinusoidal behavior. Samples fabricated on different substrates and measured with both tank coils followed closely the same behavior. It is emphasized that the experimental setup employed and the procedure followed are identical to those used to measure the current-phase relations of step-edge junctions and thin-film bicrystals with a symmetric [001] tilt of 24°. For

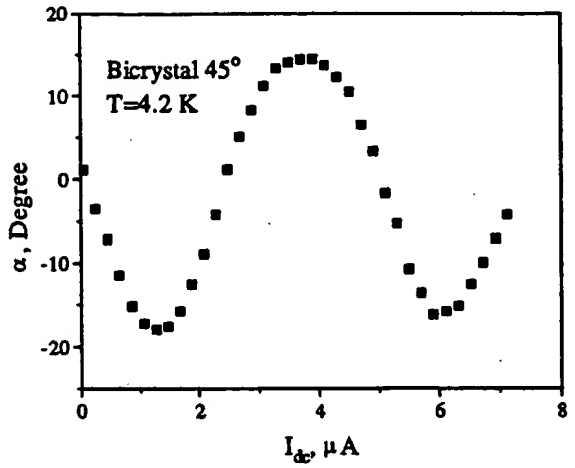

FIG. 2. Phase angle α between the driving current and the output voltage measured at 4.2 K as a function of the dc current I_{dc}, for an $YBa_2Cu_3O_{7-x}$ single junction interferometer circuit containing a symmetric 45° [001]-tilt grain boundary.

all of those samples nominally sinusoidal current-phase relations were observed, and all deviations of the apparent CPR from a sinusoidal one can be attributed to thermal noise [12,13].

The measured deviations from a sinusoidal dependence for the current-phase relations of these 45° bicrystals are startling. It is important to note that the effective Josephson penetration depth $\Lambda_J = [\Phi_0/(4\pi\mu_0\langle j_c\rangle\lambda)]^{1/2} \approx 5\ \mu$m is larger than the width of the junction b (narrow-junction limit). Here λ is the London penetration depth. Although several mechanisms are known to cause nonsinusoidal current-phase relations for narrow junctions fabricated from conventional superconductors, all of these mechanisms fail to account for the anomalous dependencies presented.

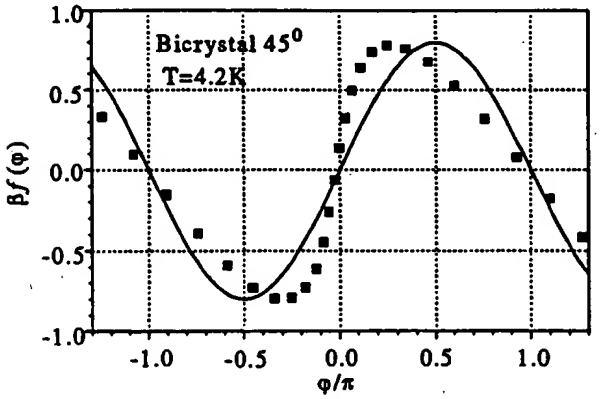

FIG. 3. The normalized current through the junction $\beta f(\varphi)$ as a function of the phase difference φ restored from the measured $\alpha(I_{dc})$ as shown in Fig. 2. For comparison, the function $\beta\sin(\varphi)$ with $\beta = 0.8$ is plotted as a solid line.

First, one potential source of such deviations is thermal noise. To evaluate its influence we consider a sinusoidal CPR and calculate with Eq. (3) the $\alpha(\varphi_{dc})$ dependence, assuming a thermally induced Gaussian spread $\rho(\varphi_n)$. With this, the value of $\tan\alpha(\varphi_{dc})$ is given by [12]

$$\tan\alpha(\varphi_{dc}) = k^2 Q\beta \times \int_{-\infty}^{\infty} \frac{\cos\varphi(\varphi_e,\varphi_n)}{1+\beta\cos\varphi(\varphi_e,\varphi_n)}\rho(\varphi_n)\,d\varphi_n . \quad (4)$$

Using Eq. (4), minor deviations of the CPR from a standard sinusoidal behavior are well described quantitatively for 24° boundaries measured at 77 K [12]. However, no realistic set of β and φ_n exists to account for the large deviations of the CPR observed for the 45° boundaries.

Second, for weak links with a high current density, current-induced suppression of the order parameter in the electrodes close to the weak link can give rise to nonharmonic current-phase relations [16]. It is unrealistic that this effect is the cause for the deviations presented here, as the intragrain critical current density exceeds 10^7 A/cm^2 at 4.2 K and is therefore much larger than the grain boundary $\langle j_c\rangle < 4000$ A/cm^2 at the same temperature.

Third, several additional mechanisms, described in [2], lead to deviations from a harmonic CPR. In all these cases, the slope of $f(\varphi)$ at $\varphi = 0$ is smaller than at $\varphi = \pi$, which is in contrast to our results. Therefore, these mechanisms cannot explain the current-phase relations observed either.

On the other hand, as will be pointed out in the following, the measured CPR can be accounted for by the unconventional order parameter symmetry of $YBa_2Cu_3O_{7-x}$ and by the microstructural properties of the grain boundaries, in particular by their faceted nature [17,18]. Interestingly, due to the $d_{x^2-y^2}$-wave character of the order parameter, the faceting has a more significant influence on the electronic properties of boundaries with a misorientation close to 45° than on boundaries with considerably smaller misorientation angles [18]. This also concerns the CPR, as the 45° boundaries contain a higher density of facets that themselves show anomalous behavior. Two kinds of such anomalies, to be considered here, are described in the literature.

First, due to the sign difference of the adjacent lobes of the $d_{x^2-y^2}$-wave order parameter, many facets are biased with an additional π phase shift (π facets) [17–19]. These phase shifts give rise to unconventional junction properties, such as a spontaneous generation of magnetic flux in the grain boundary junction [19–21]. As described in Ref. [21], the local phase difference $\varphi(x)$ along the grain boundary ($0 < x < b$) can be written as

$$\varphi(x) = \xi(x) + \psi(x), \quad (5)$$

where $\xi(x)$ is a rapidly alternating function accounting for the π phase shifts and for the spontaneously generated

magnetic flux in the junction, and $\psi(x)$ is the remaining slowly varying phase difference reflecting the magnetic flux in the interferometer loop. For a narrow junction ($b < \Lambda_J$), ψ is independent of x. With Eq. (5), the time-independent sine-Gordon equation, describing the spatial dependence of the local phase difference over the junction, becomes

$$\Lambda_J^2 \frac{\partial^2 \xi(x)}{\partial x^2} = \frac{j_c(x)}{\langle j_c \rangle} \sin[\psi + \xi(x)]. \quad (6)$$

The solution $\xi(x)$ of this equation, and thus the pattern of self-generated flux, depends on ψ. The redistribution of this flux by a change of ψ is expected to lead to remarkable deviations from a harmonic dependence for the CPR measured for the entire junction, also if the local CPR is nominally sinusoidal.

Second, it has been proposed [7,8] that the CPR of facets formed by the (110) and by the (100) planes of the adjacent grains is periodic with π and thus has a double periodicity as compared to the standard case. Transmission electron microscopy has revealed that 45° [001] tilt grain boundaries in $YBa_2Cu_3O_{7-x}$ tend to be composed for a considerable part of such facets [22]. For the whole junction, this leads to an anomalous CPR:

$$I = I_{c1} \sin\psi + I_{c2} \sin 2\psi, \quad (7)$$

by which the observed CPR can be described.

In summary, the current-phase relations of grain boundary junctions with a misorientation of 45° were measured with a modified Rifkin-Deaver method. The CPRs were deduced from measurements of the phase angle between the rf drive current and the rf tank voltage. The current-phase relations of the Josephson junctions showed pronounced deviations from a harmonic behavior, which cannot be accounted for by thermal noise or by other standard mechanisms, but are attributed to the $d_{x^2-y^2}$-wave symmetry of the order parameter and the faceting of the grain boundaries.

We are grateful to A. Golubov and M. Kupriyanov for fruitful discussions. Part of this work has been performed at the IBM Zürich Research Laboratory. Financial support by the DFG (Ho 461/1-1) and the BMBF (13N6519 and 13N6918/1) is gratefully acknowledged. One of us (H. H.) thanks the Royal Dutch Academy of Sciences and the University of Twente for their support.

[1] B. D. Josephson, Phys. Lett. **1**, 251 (1962); Rev. Mod. Phys. **36**, 216 (1964).
[2] K. K. Likharev, Rev. Mod. Phys. **51**, 101 (1979).
[3] C. C. Tsuei, J. R. Kirtley, C. C. Chi, Lock See Yu-Jahnes, A. Gupta, T. Shaw, J. Z. Sun, and M. B. Ketchen, Phys. Rev. Lett. **73**, 593 (1994).
[4] D. J. Van Harlingen, Rev. Mod. Phys. **67**, 515 (1995).
[5] D. J. Scalapino, Phys. Rep. **250**, 329 (1995).
[6] Yu. S. Barash, A. V. Galaktionov, and A. D. Zaikin, Phys. Rev. B **52**, 665 (1995).
[7] W. Zhang, Phys. Rev. B **52**, 3772 (1995).
[8] Y. Tanaka and S. Kashiwaya, Phys. Rev. B **53**, R11 957 (1996).
[9] H. Burkhardt (to be published).
[10] S. S. Tinchev, Physica (Amsterdam) **222C**, 173 (1994).
[11] V. Polushkin, S. Uchaikin, S. Knappe, H. Koch, B. David, and D. Grundler, IEEE Trans. Appl. Supercond. **5**, 2790 (1995).
[12] V. Zakosarenko, E. V. Il'ichev, R. P. J. IJsselsteijn, and V. Schultze, IEEE Trans. Appl. Supercond. **7**, 1057 (1997).
[13] E. V. Il'ichev, V. Zakosarenko, V. Schultze, H.-G. Meyer, H. E. Hoenig, V. N. Glyantsev, and A. Golubov, Appl. Phys. Lett. **72**, 731 (1998).
[14] R. Rifkin and B. S. Deaver, Phys. Rev. B **13**, 3894 (1976).
[15] D. Dimos, P. Chaudhari, J. Mannhart, and F. K. LeGoues, Phys. Rev. Lett. **61**, 219 (1988).
[16] M. Yu. Kupriyanov, Pis'ma Zh. Eksp. Teor. Fiz. **56**, 414 (1992) [JETP Lett. **56**, 399 (1992)].
[17] C. A. Copetti, F. Rüders, B. Oelze, Ch. Buchal, B. Kabius, and J. W. Seo, Physica (Amsterdam) **253C**, 63 (1995).
[18] H. Hilgenkamp, J. Mannhart, and B. Mayer, Phys. Rev. B **53**, 14 586 (1996).
[19] J. Mannhart, H. Hilgenkamp, B. Mayer, Ch. Gerber, J. R. Kirtley, K. A. Moler, and M. Sigrist, Phys. Rev. Lett. **77**, 2782 (1996).
[20] R. G. Mints and V. G. Kogan, Phys. Rev. B **55**, R8681 (1997).
[21] R. G. Mints (to be published).
[22] J. A. Alarco, E. Olsson, Z. G. Ivanov, P. A. Nilsson, D. Winkler, E. A. Stepantsov, and A. Ya. Tzalenchuk, Ultramicroscopy **51**, 239 (1993).

Dynamical Effects of an Unconventional Current-Phase Relation in YBCO dc SQUIDs

T. Lindström,[1,*] S. A. Charlebois,[1] A. Ya. Tzalenchuk,[2] Z. Ivanov,[1] M. H. S. Amin,[3] and A. M. Zagoskin[3,4]

[1]*Department of Microelectronics and Nanoscience, Chalmers University of Technology and Göteborg University, SE-412 96 Göteborg, Sweden*

[2]*National Physical Laboratory, Teddington, Middlesex TW11 0LW, United Kingdom*

[3]*D-Wave Systems Inc., 320-1985 Broadway, Vancouver, British Columbia, Canada V6J 4Y3*

[4]*Physics and Astronomy Department, The University of British Columbia, 6224 Agricultural Road, Vancouver, Canada V6T 1Z1*

(Received 20 December 2002; published 17 March 2003)

The predominant d-wave pairing symmetry in high-temperature superconductors allows for a variety of current-phase relations in Josephson junctions, which is to a certain degree fabrication controlled. In this Letter, we report on direct experimental observations of the effects of a nonsinusoidal current-phase dependence in YBCO dc SQUIDs, which agree with the theoretical description of the system.

DOI: 10.1103/PhysRevLett.90.117002 PACS numbers: 74.50.+r, 85.25.Dq

It is well established [1] that the wave function of a Cooper pair in most cuprate high-temperature superconductors (HTS) has a d-wave symmetry. Its qualitative distinction from, e.g., the anisotropic s-wave case is that the order parameter changes sign in certain directions, which can be interpreted as an *intrinsic* difference in the superconducting phase between the lobes equal to π.

The latter leads to a plethora of effects, such as formation of Andreev bound states at surfaces and interfaces in certain crystallographic orientations [2–4]. The current-phase dependence $I_S(\phi)$ in Josephson junctions formed by dd junctions, as well as by sd junctions comprised of a cuprate and a conventional superconductor, depends both on the spatial orientation of the d-wave order parameter with respect to the interface, and on the quality of the latter [5–9]. Time-reversal symmetry can also be spontaneously violated and thus spontaneous currents generated [10–12]. Another effect can be doubling of the Josephson frequency [6,13,14].

In this Letter, we report on experimental observations of strong effects of an unconventional current-phase relation on the dynamics of two dd junctions integrated into a superconducting interference device (SQUID) configuration.

Since $I_S(\phi)$ must be a 2π-periodic odd function, it can be expanded in a Fourier series. In most cases, only the first two harmonics give a significant contribution to the current:

$$I_S(\phi) = I_c^{\mathrm{I}} \sin\phi - I_c^{\mathrm{II}} \sin 2\phi. \quad (1)$$

In Josephson systems of conventional superconductors, the second harmonic will usually be negligible [15] but in dd junctions the second harmonic may dominate. If $I_c^{\mathrm{II}} > I_c^{\mathrm{I}}/2$, the equilibrium state is no longer $\phi = 0$ but becomes double degenerate at $\phi = \pm \arccos(I_c^{\mathrm{I}}/2I_c^{\mathrm{II}}) \to \pm\pi/2$. The system can then spontaneously break time-reversal symmetry by choosing either state. Spontaneous currents as well as fluxes can be generated in this state. The potential will have the shape of a double well, and there are reasons to believe that it will be possible to observe quantum coherence in this system. The presence of a second harmonic in the current-phase relation (CPR) of a dd junction was confirmed by Il'ichev *et al.* [8].

A nonsinusoidal CPR of the junctions will change the dynamics of a dc SQUID [16]. Regarding the junctions as magnetically small, the supercurrent through the SQUID in the presence of an external flux $\Phi_x \equiv \Phi_0 \cdot (\phi_x/2\pi)$ can be written as

$$I_s(\phi, \phi_x) = I_{c1}^{\mathrm{I}} \sin\phi - I_{c1}^{\mathrm{II}} \sin(2\phi) + I_{c2}^{\mathrm{I}} \sin(\phi + \phi_x) - I_{c2}^{\mathrm{II}} \sin 2(\phi + \phi_x). \quad (2)$$

The critical current through the SQUID is given by the usual expression $I_c(\phi_x) = \max_\phi I_s(\phi, \phi_x)$. The time-averaged voltage over the SQUID in the resistive regime is readily obtained in the resistively shunted junction approximation. By introducing $\delta[\phi, \phi_x] = \phi_2 - \phi_1$ and applying the same method as in [17] with the necessary generalizations, we obtain the following for the average voltage over the SQUID:

$$\overline{V}^{-1} = \frac{G_1 + G_2}{2\pi} \int_{-\pi}^{\pi} d\phi \left[I - (G_1 - G_2)\frac{\hbar}{2e}\frac{d\delta}{dt} - I_1\left(\phi + \frac{\delta}{2}\right) - I_2\left(\phi - \frac{\delta}{2}\right)\right]^{-1}. \quad (3)$$

Here $G_{1,2}$ are the normal conductances of the junctions, and

$$\delta + \phi_x + \frac{\pi L}{\Phi_0}[I_2(\phi - \delta/2) - I_1(\phi + \delta/2)] = 0 \quad (4)$$

gives the difference, δ, in phase drops across each junction. In deriving (3) and (4), we have assumed that the inductance L is equally divided between the SQUID arms. We have also neglected the spontaneous magnetic fluxes in the dd junctions, due to their small amplitude [11,18]. Though (4) is only explicitly solvable in the limit

$L \to 0$, it always yields $\delta[-\phi, -\phi_x] = -\delta[\phi, \phi_x]$. This means that the usual inversion symmetry is retained.

The results of numerical calculations based on (2) and (3) are shown in Fig. 1. The cusps in the critical current correspond to the points at which the global maximum in (1) switches from one local maximum to another [16]. Note the quasi-$\Phi_0/2$ periodicity of the current isolines in the $\bar{V} - \phi_x$ picture, reflecting the current-phase dependence (1), and their shift along the Φ_x axis, which depends on the sign of the bias current (as it must to maintain the central symmetry with respect to the origin). The shift does not depend on the magnitude of the current since we neglect the self-inductance. For large biases, the Φ_0 periodicity is restored. Indeed, as the bias grows, one set of minima of the washboard potential, $U = (h/2e)[-I^{\mathrm{I}}\cos\phi + (I^{\mathrm{II}}/2)\cos 2\phi - I\phi]$, disappears first unless the first harmonic I^{I} is *exactly* zero.

We have fabricated and studied a large number of dc SQUIDs. The samples were fabricated from 250 nm thick YBCO films deposited on $SrTiO_3$ bicrystals. The grain-boundary junctions (GBJs) are of the asymmetric [001]-tilt type with the misorientation angle of 45° (0°–45° GBJ). For more information on GBJs see, for example, Ref. [19].

The pattern was defined using *E*-beam lithography and then transferred to a carbon mask employing a multistep process. Finally, the YBCO is etched through the mask using ion milling. This scheme allows us to fabricate high-quality bicrystal junctions as narrow as 0.2 μm, as has been reported elsewhere [20]. In the SQUIDs under investigation, the junctions are nominally 2 μm wide; hence, the fabrication-induced damage of the junctions is small.

The measurements were done in an EMC-protected environment using a magnetically shielded LHe cryostat. However, the magnetic shielding is imperfect, as is evident from the fact that the expected zero-field response of our SQUIDs is not exactly at zero. The measuring electronics is carefully filtered and battery powered whenever possible. In order to measure the dependence of the critical current on the applied field, we used a voltage discriminator combined with a sample-and-hold circuit. All measurements reported here were performed at 4.2 K.

The SQUID loops are (15 × 15) μm^2. The numerically calculated inductance [21] is approximately 25 pH, yielding the factor $\beta = 2\pi L I_c/\Phi_0$ between 0.5–2.

The SQUIDs were largely nonhysteretic with a resistance of about 2 Ω. The measured critical current varies from sample to sample but is in the range of tens of microamperes giving a current density of the order of $J_c = 10^3$ A/cm^2. The estimated Josephson penetration length $\lambda_J = \Phi_0/\sqrt{4\pi\mu_0 j_c \lambda_L}$ is approximately 2 μm in all junctions, which means that the junctions are magnetically short. This is supported by the quasiperiod of the pattern in Fig. 2 being close to the expected value $\phi_0/2\lambda_L w$ [17]. The differential conductance curves do not show any trace of a zero bias anomaly (ZBA), as is expected for 0°–45° GBJs. ZBAs have been observed by other groups in GBJs with other orientations [2].

The critical current is plotted as a function of applied magnetic field for two SQUIDs in Fig. 3. The result is in qualitative agreement with theory if we assume that the SQUID junctions have different ratios of the first and second harmonics of the critical current. This assumption

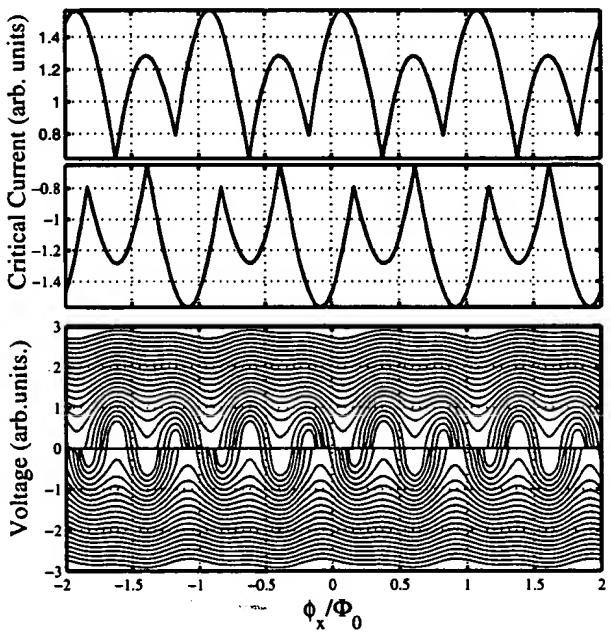

FIG. 1. The results of simulations of the $I_c - \phi_x$ and $\bar{V} - \phi_x$ dependence for a dc SQUID with $I^{\mathrm{I}}_{c1} = 1$, $I^{\mathrm{I}}_{c2} = 0.1$, $I^{\mathrm{II}}_{c1} = 0.2$ and $I^{\mathrm{II}}_{c2} = 0.4$ (arbitrary units). The different curves correspond to bias currents in the range $I = I^{\mathrm{I}}_{c1}$ to $I = 5I^{\mathrm{I}}_{c1}$. We assume $L = 0$ and $G_1 = G_2$.

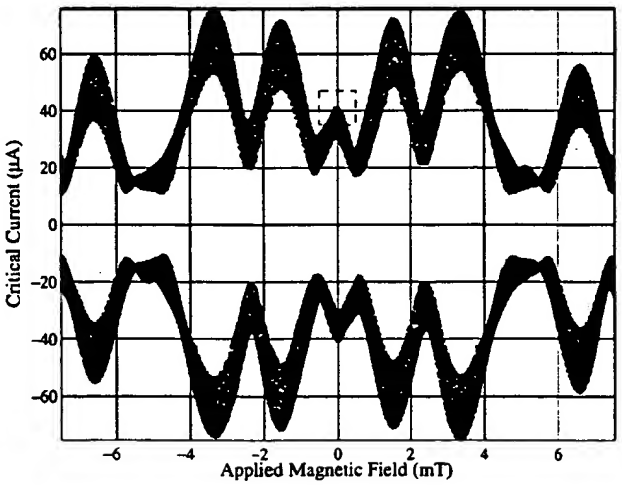

FIG. 2. Critical current as a function of magnetic field at 4.2 K. The dashed box indicates the area plotted in Fig. 3(a).

is supported by the fairly small modulation depth [it is easy to see from Eq. (2) that I_c would go exactly to zero in a SQUID with junctions of identical I_{c2}/I_{c1}].

We can fit the data to Eq. (2), if we compensate for the residual background magnetic field and assume that we have a small excess current (of the order of a few μA) in the junctions. The fitting parameters again confirm that there is a large asymmetry between the arms of the SQUIDs. Note that the model does not consider the flux penetration into the junctions,

The result for fields of the order of mT is presented in Fig. 2, which shows the I_c modulation of the SQUID enveloped by an anomalous Fraunhofer pattern quite similar to what has been reported by other groups [22,23] for 0°–45° GBJs. Note the inversion symmetry of the pattern with respect to the origin. That the global maximum is not in the center can be explained in several ways; it has been shown, for example, that this could be due to the presence of so-called π loops in the junction interface [24].

Figure 4 shows the V-B dependence of one of the SQUIDs. The pattern is again field inversion symmetric. The overall structure is the same as in the model dependence of Fig. 1, but there is also an additional shift due to self-field effects, which depends on the magnitude of the bias current and corresponds (at maximum) to a flux $\sim 0.1\Phi_0$. In a beautiful experiment, a similar dependence was recently observed by Baselmans *et al.* in a Nb-Ag-Nb SNS junction where current injectors were used to change the occupation of current-carrying states in the normal region [25]. A deviation from the model occurs at $\overline{V} = 100\ \mu$V where the minima and maxima switch. This is probably due to an LC resonance in the SQUID. Taking $L = 25\ pH$, this would require $C = 0.8\ pF$, which agrees with our measurements on single junctions

Remarkably, the observed offset of the V-B characteristics with respect to the *direction* of the bias current appears to be a much more robust manifestation of the presence of a second harmonic of the Josephson current than the shape of the $I_c - B$ curves itself. We observed the shift even in SQUIDs with the smallest junctions down to 0.5 μm wide, where the deviations from the usual sinusoidal CPR were not obvious from the $I_c - B$ dependence.

Generally, the nature of the transport through a GBJ will depend on its transmissivity D. Il'ichev *et al.* [8] have reported values of D as high as 0.3 in symmetric (22.5°–22.5°) *dd* junctions as opposed to the usual estimate for a GBJ, $D \sim 10^{-5}$–10^{-2}. Since usually $I_c^{II}/I_c^{I} \propto D$, a high-transmissivity GBJ is required in order

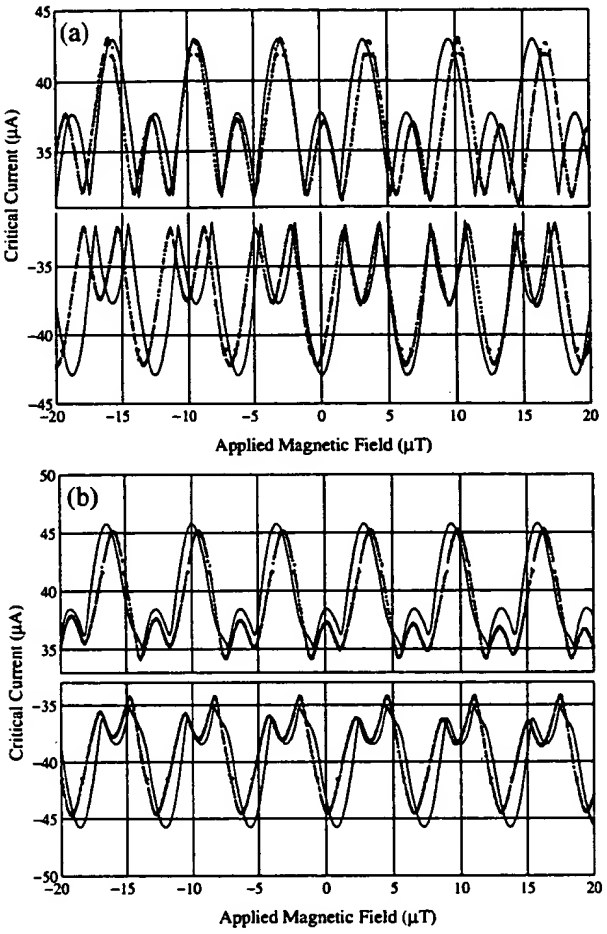

FIG. 3. Critical current as a function of applied magnetic field for two different SQUIDs that are nominally identical. The solid line represents the fitted expression. The fitting parameters are as follows: (a) $I_{c1}^{I} = 9\ \mu$A, $I_{c2}^{I} = 0.3\ \mu$A, $I_{c1}^{II} = 3.7\ \mu$A, and $I_{c2}^{II} = 22.7\ \mu$A; (b) $I_{c1}^{I} = 7.8\ \mu$A, $I_{c2}^{I} = 3.0\ \mu$A, $I_{c1}^{II} = 5.3\ \mu$A, and $I_{c2}^{II} = 4.3\ \mu$A. In both cases, the fit has been adjusted with respect to the residual background field and the excess current of the junctions.

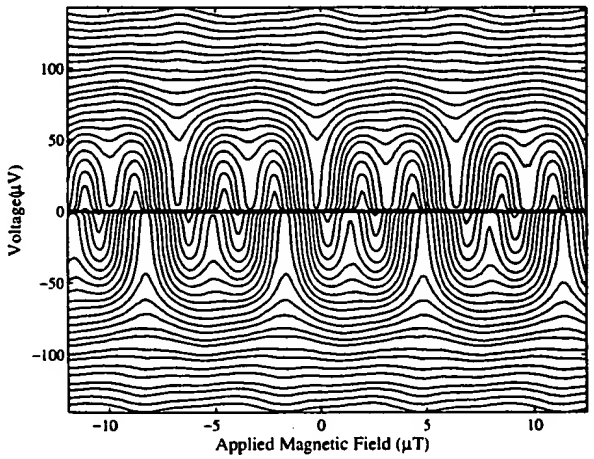

FIG. 4. Voltage modulation as a function of applied magnetic field for the SQUID whose $I_c - B$ is shown in Fig. 3(a). The pattern is again inversion symmetric. Note the sign change at 100 μV, which we believe is due to a LC resonance in the SQUID loop.

to observe effects of the second harmonic. An estimate of the *average* transmissivity of our junctions would be $\rho_{ab}l/R_NA \sim 10^{-2}$ [26] assuming l, the mean-free path, to be equal to 10 nm and a resistivity in the a-b plane ρ_{ab} equal to $10^{-4}\ \Omega$ cm. This is still too low to explain the strong second harmonic we observe. However, it is known from, e.g., TEM studies [19], that the grain-boundary is far from uniform; the properties can significantly vary depending on the local properties of the interface, effects such as oxygen diffusion out of the GB, etc., which are difficult to control. It is therefore reasonable to assume that there are many parallel transport channels through the GB [27,28]. Channels with high-transmissivity dominate the transport and might have $D \sim 0.1$ even though the *average* transmissivity is much lower. This is also consistent with the fact that most of our SQUIDs seem to be highly asymmetrical which is to be expected if the distribution of channels is random. The ratios of I_c^{I} and I_c^{II} can vary as much as 10 times between two junctions in the same SQUID, even though the fluctuations of the *total* I_c from sample to sample are much smaller. It is also clear from general considerations that a high value of I_c^{II} *excludes* a high value of I_c^{I}, since the second harmonic usually dominates if the odd harmonics of the supercurrent are canceled by symmetry [29].

Recent studies of 0°–45° GBJs have demonstrated that the SQUID dynamics can be altered by the d-wave order parameter in YBCO [30]. It is, however, important to point out that our results *do not* directly relate to, e.g., tetracrystal π-SQUID experiments; the latter crucially depend on having one π junction with negative critical current, but still only the first harmonic present in $I_c(\phi)$. Our SQUIDs have a conventional geometry, but unconventional current-phase relations.

One explanation for the pronounced effects of the second harmonic could be that relatively large sections of the interface are highly transparent and have a low degree of disorder. This in turn could be related to our fabrication scheme which seems to preserve the integrity of the barrier. This makes feasible their applicability in the quantum regime and supports our expectations that quantum coherence can be observed in this kind of structures.

In summary, we have observed a very pronounced second harmonic in the current-phase relation of a "conventional" YBCO dc SQUID with 0°–45° grain-boundary junctions. It has strongly influenced the SQUID dynamics. All details of the SQUID behavior were explained within a simple model of a *dd* junction with relatively high transparency. We believe that these effects are important for better understanding of HTS Josephson junction and SQUIDs.

Discussions with Evgeni Il'ichev, Alexander Golubov, Tord Claeson, and John Gallop are gratefully acknowledged. The work is in part supported by The Board for Strategic Research (SSF) via the "OXIDE" program, the Science Research Council, and the "Fonds québécois de la recherche sur la nature et les technologies." The processing work is done at the MC2 process laboratory at Chalmers University of Technology.

*Electronic address: tobiasl@fy.chalmers.se

[1] C. Tsuei and J. Kirtley, Rev. Mod. Phys. **72**, 969 (2000).
[2] L. Alff *et al.*, Phys. Rev. B **58**, 11 197 (1998).
[3] T. Löfwander, V. Shumeiko, and G. Wendin, Supercond. Sci. Technol. **14**, R53 (2001).
[4] C.-R. Hu, Phys. Rev. Lett. **72**, 1526 (1994).
[5] S. Yip, Phys. Rev. B **52**, 3087 (1994).
[6] A. Zagoskin, J. Phys. Condens. Matter **9**, L419 (1997).
[7] E. Il'chev *et al.*, Phys. Rev. B **60**, 3096 (1999).
[8] E. Il'ichev *et al.*, Phys. Rev. Lett. **86**, 5369 (2001).
[9] P. Komissinski *et al.*, Europhys. Lett. **57**, 585 (2002).
[10] A. Huck, A. van Otterlo, and M. Sigrist, Phys. Rev. B **56** 14163 (1997).
[11] M. H. S. Amin, A. N. Omelyanchouk, and A. M. Zagoskin, Phys. Rev. B **63**, 212502 (2001).
[12] S. Östlund, Phys. Rev. B **58**, R14 757 (1998).
[13] T. Löfwander, G. Johansson, M. Hurd, and G. Wendin, Phys. Rev. B **57**, R3225 (1998).
[14] H. Arie *et al.*, Phys. Rev. B **62**, 11 864 (2000).
[15] M. Keene, C. Gough, and A. Rae, J. Phys. Condens. Matter **3**, 6079 (1991).
[16] M. H. S. Amin, M. Coury, and R. Rose, IEEE Trans. Appl. Supercond. **12**, 1877 (2002).
[17] A. Barone and G. Paterno, *Physics and Applications of the Josephson Effect* (Wiley, New York, 1982).
[18] M. H. S. Amin, S. N. Rashkeev, M. Coury, A. N. Omelyanchouk, and A. M. Zagoskin, Phys. Rev. B **66**, 174515 (2002).
[19] H. Hilgenkamp and J. Mannhart, Rev. Mod. Phys. **74**, 297 (2002).
[20] A. Tzalenchuk *et al.*, Appl. Phys. Lett. (to be published).
[21] M. Khapaev, A. Kidiyarova-Shevchenko, P. Magnelind, and M. Kupriyanov, IEEE Trans. Appl. Supercond. **11**, 1090 (2001).
[22] J. Mannhart, B. Mayer, and H. Hilgenkamp, Z. Phys. B **101**, 175 (1996).
[23] W. Neils and D. van Harlingen, Physica (Amsterdam) **284B–288B**, 587 (2000).
[24] H. Smilde *et al.*, Phys. Rev. Lett. **88**, 057004 (2002).
[25] J. Baselmans, T. Heikkilä, B. van Wees, and T. Klapwijk, Phys. Rev. Lett. **89**, 207002 (2002); the pronounced second harmonic in this experiment appears due to nonequilibrium effects, see, e.g., J. C. Clarke, in *Nonequilibrium Superconductivity, Phonons and Kapitza Boundaries*, edited by K. E. Gray, NATO ASI Series (Plenum, New York, 1981), p. 353.
[26] G. Blonder, M. Tinkham, and T. Klapwijk, Phys. Rev. B **25**, 4515 (1982).
[27] Y. Naveh, D. Averin, and K. Likharev, Phys. Rev. Lett. **79**, 3482 (1997).
[28] E. Sarnelli, G. Testa, and E. Esposito, J. Supercond. **7**, 387 (1994).
[29] Y. Barash, Phys. Rev. B **61**, 678 (2000).
[30] B. Chesca *et al.*, Phys. Rev. Lett. **88**, 177003 (2002).

Feasibility of biepitaxial $YBa_2Cu_3O_{7-x}$ Josephson junctions for fundamental studies and potential circuit implementation

F. Tafuri
Dipartimento di Ingegneria dell'Informazione, Seconda Università di Napoli, 81031 Aversa (CE) and
INFM-Dipartimento Scienze Fisiche dell'Università di Napoli "Federico II", 80125 Napoli (ITALY)

F. Carillo, F. Lombardi, F. Miletto Granozio, F. Ricci, U. Scotti di Uccio and A. Barone
INFM-Dipartimento Scienze Fisiche dell'Università di Napoli "Federico II", 80125 Napoli (ITALY)

G. Testa and E. Sarnelli
Istituto di Cibernetica del CNR, Via Toiano 6, Arco Felice (NA) (ITALY) also INFM

J.R. Kirtley
IBM T.J. Watson Research Center, P.O. Box 218, Yorktown Heights, NY 10598, USA

(July 4, 2003)

We present various concepts and experimental procedures to produce biepitaxial $YBa_2Cu_3O_{7-x}$ grain boundary Josephson junctions. The device properties have an interesting phenomenology, related in part to the possible influence of "π-loops". The performance of our junctions and Superconducting Quantum Interference Devices indicates significant improvement in the biepitaxial technique. Further, we propose methods for fabricating circuits in which "0-" and "π-loops" are controllably located on the same chip.

I. INTRODUCTION

The possibility of realizing electronic circuits in which the phase differences of selected Josephson junctions are biased by π in equilibrium is quite stimulating.[1] The concept of such π-phase shifts was originally developed in the "extrinsic" case for junctions with ferromagnetic barriers[2] and in the "intrinsic" case for junctions exploiting superconductors with unconventional order parameter symmetries.[3] As a result of the possible $d_{x^2-y^2}$ order parameter symmetry of high critical temperature superconductors (HTS),[4] the presence of intrinsic π loops has also been considered for HTS systems.[5] This has been discussed recently in view of novel device concepts, and in particular for the implementation of a solid state qubit[1,6–8] and for Complementary Josephson junction electronics.[9] In this paper we discuss how $YBa_2Cu_3O_{7-x}$ (YBCO) structures made by the biepitaxial technique[10,11] can be successfully employed to produce arbitrary circuit geometries in which both "0" and π-loops are present, and possibly to obtain a doubly degenerate state.[1,6] Of course, great caution should be used because of stringent requirements on junctions parameters for practical applications of such devices.

Josephson junctions based on artificially controlled grain boundaries have been widely employed for fundamental studies on the nature of HTS.[4,7,8] The lack of a reliable technology based on the traditional trilayer configuration (i.e. a sandwich type junction with an insulator between the two superconducting electrodes) also enhanced interest in GB Josephson junctions for applications. Although the mechanism of high-T_C superconductivity and the influence of grain boundaries on the transport properties are not completely determined, reproducible and good quality devices are routinely fabricated. YBCO GB junctions are usually classified as bicrystals,[12] biepitaxials,[11] and step-edges,[13] depending on the fabrication procedure. The bicrystal technique typically offers junctions with better performances and allows in principle the realization of all different types of GBs ranging from [001] and [100] tilt to [100] twist boundaries. GB junctions based on the step-edge and biepitaxial techniques offer the advantage, with respect to the bicrystal technology, of placing the junctions on the substrate without imposing any restrictions on the geometry. A comparison between the different GB techniques is far beyond the aim of this paper. Nevertheless we intend to show that significant improvements with respect to the original technique developed by Char et al.[11] are possible for biepitaxial junctions, and that the resulting devices have potential for applications. As a matter of fact, in traditional biepitaxial junctions, the seed layer used to modify the YBCO crystal orientation on part of the substrate produces an artificial 45° [001] tilt (c-axis

tilt) GB. The nature of such a GB seems to be an intrinsic limit for some real applications. A convincing explanation has been given in terms of the d-wave nature of the order parameter and more specifically by the presence of π-loops.[14] As demonstrated by studies on bicrystals, based on the same type of 45° [001] tilt GB, the presence of π -loops reduces the $I_C R_N$ values (where I_C and R_N are the critical current and the high normal state resistance respectively), produces a dependence of the critical current I_C on the magnetic field H quite different from the Fraunhofer-like pattern, and generates unquantized flux noise at the grain boundary.[14]

We will show that the implementation of the biepitaxial technique[10] we developed to obtain 45° [100] tilt and twist (a-axis tilt and twist) GBs junctions makes such a technique interesting for both applications and fundamental studies. The phenomenology observed for the junctions based on these GBs and Scanning SQUID Microscopy investigations demonstrate the absence of π-loops, as we expect from their microstructure. As a consequence higher values of the $I_C R_N$ values, a Fraunhofer like dependence of I_C on the magnetic field and lower values of the low frequency flux noise, when compared with 45° c-axis tilt GBs, have been measured. These features are important tests to employ junctions for applications. Scanning SQUID Microscopy investigations also gave evidence of "fractional" vortices in the presence of impurities. Finally, we extended the biepitaxial process to other types of GB by using different seed layers to obtain junction configurations where π loops can be controllably produced. We shall not dwell on conceptual principles and actual feasibility of qubit devices. Instead we discuss the importance of the biepitaxial technique in having "0" and "π" loops on the same chip. This makes the biepitaxial technique more versatile and promising for circuit design.

II. DEVICES: CONCEPTS AND FABRICATION PROCEDURE

As mentioned above, the biepitaxial technique allows the fabrication of various GBs by growing different seed layers and using substrates with different orientations. We have used MgO, CeO_2 and $SrTiO_3$ as seed layers. The MgO and CeO_2 layers are deposited on (110) $SrTiO_3$ substrates, while $SrTiO_3$ layers are deposited on (110) MgO substrates; in all these cases the seed layers grow along the [110] direction. Ion milling is used to define the required geometry of the seed layer and of the YBCO thin film respectively, by means of photoresist masks. YBCO films, typically 120nm in thickness, are deposited by inverted cylindrical magnetron sputtering at a temperature of 780° C. YBCO grows along the [001] direction on MgO (substrates or seed layers) and on the CeO_2 (seed layers), while it grows along the [103]/[013] direction on $SrTiO_3$ (substrates or seed layers). In order to select the [103] or [$\bar{1}$03] growth and to ensure a better structural uniformity of the GB interface, we have also successfully employed vicinal substrates. However, most of the transport properties presented in this paper refer to samples not using vicinal substrates. Detailed structural investigations on these GBs, including Transmission Electron Microscopy (TEM) analyses, have been performed and the results have been presented elsewhere.[10,16]

Depending on the patterning of the seed layer and the YBCO thin film, different types of GBs ranging from the two ideal limiting cases of 45° a-axis tilt and 45° a-axis twist have been obtained (see Fig.1). The intermediate situation occurs when the junction interface is tilted at an angle α different from 0 or $\pi/2$ with respect to the a- or b-axis of the [001] YBCO thin film. In all cases, the order parameter orientations do not produce an additional π phase shift along our junction, in contrast with the 45° asymmetric [001] tilt junctions. As a consequence, no π loops should occur independently of the details of the interface orientation. In Fig. 1 we consider ideal interfaces and neglect meandering of the GBs or interface anomalies that will be considered below. The CeO_2 seed layer may produce a more complicated GB structure, in which a 45° c-axis tilt accompanies the 45° a-axis tilt or twist (see Fig.2a).[15] In this case, as shown in Fig.2b, π loops should occur in analogy with the traditional biepitaxial junctions based on 45° c-axis tilt GBs. In both Figs. 1 and 2 we display the possible $d_{x^2-y^2}$ -wave order parameter symmetry in the junction configuration. Junctions were typically 4 microns wide. We also performed systematic measurements on SQUIDs based on the structure employing MgO as a seed layer and $SrTiO_3$ as a substrate. DC SQUIDs in different configurations and with loop inductance typically ranging from 10 to 100 pH have been investigated. The typical loop size leading to the 10(100) pH inductance is approximately $10^2\mu m^2$ ($10^4\mu m^2$).

III. EXPERIMENTAL RESULTS

A. Biepitaxial junctions employing MgO seed layers

In this section we attempt to cover most of the phenomenology of the transport properties of 45° a-axis tilt and twist biepitaxial junctions. In Fig. 3, current vs voltage (I-V) characteristics of a typical biepitaxial junction are given for various temperatures close to the critical temperature. In the inset the corresponding I-V characteristic at T = 4.2 K is reported. They are closely described by the resistively-shunted-junction (RSJ) model and no excess current is observed. Nominal critical current densities J_C of 5 x 10^2A/cm^2 at T = 77 K, and of 9 x 10^3A/cm^2 at T = 4.2 K have been measured respectively. The R_N value (3.2 Ω) is roughly independent of the temperature for $T < T_C$, providing a normal state specific conductance $\sigma_N = 70\ (\mu\Omega cm^2)^{-1}$. The maximum working temperature T_C of this device was 82 K. In this case

$I_C R_N$ is 1.3 mV at T = 4.2 K. These values typically ranged from 1 mV to 2 mV at T = 4.2 K. They are larger for the corresponding J_C values than those provided by conventional biepitaxials, and are of the same order of magnitude as in GB bicrystal and step edge junctions.[10] While the values of critical current density and normal state specific conductance in the tilt case are quite different from the twist case, the $I_C R_N$ values are approximately the same for both. Moreover $I_C R_N$ does not scale with the critical current density.[10] In the tilt cases $J_C \approx$ 0.5-10 10^3 A/cm^2 and $\sigma_N \approx$ 1-10 $(\mu\Omega\text{cm}^2)^{-1}$ are measured at T = 4.2 K respectively. Twist GBs junctions are typically characterized by higher values of J_C in the range 0.1-4.0 x 10^5 A/cm^2 and of σ_N in the range 20-120 $(\mu\Omega\text{cm}^2)^{-1}$ (at T = 4.2 K). For the twist case deviations from the RSJ model are more marked as a result of higher critical current densities. For high values of J_C GB junctions do not present any clear modulation of the critical current as a function of the magnetic field.

A demonstration of the possibility of tailoring the critical current density and of the different transport regimes occurring in the tilt and twist cases has been given by measuring the properties of junctions with different orientations of the GB barrier on the same chip. By patterning the seed layer as shown in Fig.4a, we could measure the properties of a tilt junction and of junctions whose interface is tilted in plane by an angle $\alpha = 30°$, 45° and 60° with respect to the a- or b-axis of the [001] YBCO thin film respectively. In all cases the order parameter orientations do not produce an additional π phase shift along our junction, in contrast with the 45° [001] tilt junctions, and no π loops should occur. We measured the expected increase of the critical current density with increasing angle, which corresponds on average to an increase of the twist current component. The values measured at T = 4.2 K are reported in Fig. 4a and range from the minimum value $J_C = 3 \times 10^2$ A/cm^2 in the tilt case to the maximum $J_C = 10^4$ A/cm^2 corresponding to an angle of 60°, for which the twist component is higher. The consistency of this result has been confirmed by the values of normal state resistances, which are higher in the tilt case and decrease with increasing α. The $I_C R_N$ values are about the same for all the junctions independently of the angle α. In Fig. 4b the I-V characteristics measured at T = 4.2 K, corresponding to the junctions of Fig.4a, are shown for approximately the same voltage range. Deviations from RSJ behavior appear for higher values of the critical current density ($\alpha = 60°$). These results demonstrate that the grain boundary acts as a tunable barrier. This possibility of modifying the GB macroscopic interface plane by controlling the orientation of the seed layer's edge is somehow equivalent to the degree of freedom offered by bicrystal technology to create symmetric or asymmetric GBs, with the advantage of placing all the junctions on the same substrate. The 45° a-axis tilt and twist GBs and the intermediate situations can represent ideal structures to investigate the junction physics in a wide range of configurations. The anisotropy of the (103) films and the possibility to select the orientation of the junction interface by suitably patterning the seed layer, and eventually the use of other seed layers which produce different YBCO in plane orientations, allow the fabrication of different types of junctions and the investigation of different aspects of HTS junction phenomenology. In particular we refer to the possibility of changing the tunneling matrix elements (by selecting the angle α) and to use the anisotropy of the layered structure of YBCO properties and of the order parameter symmetry.

The study of the junction properties in the presence of an external magnetic field H is a fundamental tool for the investigation of the Josephson effect in the various junctions, as well as a test of junction quality.[17] We observe modulations of the critical current I_C following the usual Fraunhofer-like dependence. The I_C (H) patterns are mostly symmetric around zero magnetic field, and in all samples the absolute maximum of I_C occurs at H=0. The presence of the current maximum at zero magnetic field is consistent with the fact that in our junction configuration the order parameter orientations do not produce an additional π phase shift, in contrast with the 45° [001] tilt GB junctions.[14,10] Some examples are given in Fig. 5, where the magnetic pattern relative to a SQUID and a single junction at T = 4.2 K are shown respectively. In the former case we can also distinguish a smaller field modulation (with a period of 8 mG) which corresponds to the SQUID modulation (inset a). In the latter case the I-V characteristics are reported for different magnetic fields (inset b). Despite the Fraunhofer-like dependence, some deviations are evident, in agreement with most of the data available in literature.

For sake of completeness we also acknowledge some work we carried out by investigating Fiske steps as a function of H in other junctions, giving some evidence of a dielectric-like behavior[18] of some of the layers at the junction interface. We already reported about this work elsewhere.[19] The Fiske steps do not depend on the use of a particular substrate, since they have been observed in junctions based both on $SrTiO_3$ and MgO substrates. Typical values of the ratio between the barrier thickness t and the relative dielectric constant ϵ_r range from 0.2 nm to 0.7 nm. Considerations on the dependence of I_C on the temperature (T) can be also found in Ref.[19]. In junctions characterized by lower critical current densities, I_C tends to saturate at low temperatures, in contrast to those characterized by higher critical currents, for which there is a linear increase.[10,20]

B. Scanning SQUID microscopy on biepitaxial junctions with MgO seed layer

Figure 6 is a scanning SQUID microscope[21] image of a 200x200μm^2 area along a grain boundary separating a (100) region from a (103) region (as labelled in the figure) of a thin YBCO biepitaxial film grown as described

above. The position of the grain boundary is indicated by the dashed line. The image was taken at 4.2K in liquid helium with an octagonal SQUID pickup loop 4 microns in diameter after cooling the sample in a few tenths of a μT externally applied magnetic field normal to the plane of the sample. The grey-scaling in the image corresponds to a total variation of $0.13\Phi_0$ of flux through the SQUID pickup loop. Visible in this image are elongated interlayer Josephson vortices in the (103) area to the right, and "fractional" vortices in the (100) area to the left, of the grain boundary. Fits to the interlayer vortices give a value for the c-axis penetration depth of about 4μm. The "fractional" vortices are spontaneously generated in the (100) film, regardless of the value of external field applied.[22] Temperature dependent scanning SQUID microscope imaging shows that this spontaneous magnetization, which appears to be associated with defects in the film, arises when the film becomes superconducting.[4,23] Although it is difficult to assign precise values of total flux to the "fractional" vortices, since they are not well separated from each other, fits imply that they have less than Φ_0 of total flux in them, an indication of broken time-reversal symmetry. Although there is apparently some flux generated in the grain boundary region, the fact that these SQUIDs have relatively low noise seems to indicate that this flux is well pinned at the temperatures at which the noise measurements were made. These results are consistent with the absence of π loops along the grain boundary.

C. Biepitaxial junctions employing CeO_2 seed layers

The CeO_2 seed layer, as anticipated in section II, may produce an artificial GB that can be seen as a result of two rotations: a 45° [100] tilt or twist followed by a 45° [001] tilt around the c-axis of the (001) film. For this junction configuration a d-wave order parameter symmetry would produce π-loops, as shown in Fig. 2. We notice that such π-loops are structurally different from those usually obtained by the 45° [001] tilt GB junctions based on the traditional biepitaxial and bicrystal techniques. Due to the microstructure we expect especially in the [100] tilt case low critical current densities and high normal state resistances. We found that the deposition conditions to select the uniform growth of YBCO 45° tilted around the c-axis of the (001) film are critical. Preliminary measurements realized on tilt-type junctions with a CeO_2 seed layer gave evidence of Josephson coupling in these GBs. The measured I_CR_N values are from 200 μV to 750 μV and are in the typical range of the GBs Josephson junctions.

D. Biepitaxial SQUIDs employing MgO seed layers

In this section we report on the characterization of dc-SQUIDs which are to our knowledge the first employing the GBs discussed above.[24] These SQUIDs exhibit very good properties, and noise levels which are among the lowest ever reported for biepitaxial junctions.[24] Apart from implications for applications, these performances are important for the study of the transport properties of HTS Josephson junctions. In Fig. 7 we show the magnetic field dependence of the voltage at 77 K for different values of the bias current for a dc-SQUID with an inductance of 13 pH. At this temperature I_CR_N is about 20 μV. The corresponding value of the screening parameter β=$2LI_C/\Phi_O$ is 0.03. In general low β values are mandatory to avoid the influence of asymmetric inductances in SQUID properties, and this has been crucial for experiments designed to study the order parameter symmetry.[7] The presented curves are quite typical. These SQUIDs usually work in a wide temperature range from low temperatures (4.2 K) up to temperatures above 77 K. The maximum working temperature was in this case 82 K. The achieved magnetic flux-to-voltage transfer functions $V_\Phi = \partial V/\partial\Phi$, where V and Φ are the voltage across the device and the applied magnetic flux in the SQUID loop respectively, are suitable for applications. For instance at T = 77 K an experimental value of the SQUID amplitude voltage modulation ΔV of 10.4 mV was measured, corresponding to $V_\Phi = 36.9\ \mu V/\Phi_0$.[24] Steps of different nature have been recurrently observed in the I-V characteristics in the washer and hole configurations and characterized also in terms of the magnetic field dependence of the voltage at different values of the bias current.

The noise spectral densities of the same dc-SQUID have been measured at T = 4.2 K and T = 77 K using standard flux-locked-loop modulated electronics. The energy resolution $\epsilon = S_\Phi/2L$ (with S_Φ being the magnetic-flux-noise spectral density) at T = 4.2 K and T = 77 K is reported in Fig. 8. At T = 4.2 K and 10 kHz, a value of $S_\Phi = 3\ \mu\Phi_0/\sqrt{Hz}$ has been measured, corresponding to an energy resolution $\epsilon = 1.6\text{x}10^{-30}$ J/Hz. This value is the lowest reported in the literature for YBCO biepitaxial SQUIDs. Moreover, the low frequency 1/f flux noise spectral density at 1 Hz is more than one order of magnitude lower than the one reported for traditional biepitaxials, as is also evident from the comparison with data at T = 4.2 K of Ref.[25]. The lower values of low frequency noise are consistent with the absence of π-loops on the scale of the faceting for these types of GBs, as clearly shown by Scanning SQUID Microscopy results. The π-loops produce some types of spontaneous magnetic flux in the GB region, which among other effects tends to degrade the SQUID's noise levels.[14]

IV. BIEPITAXIAL JUNCTIONS FOR EXPERIMENTS ON THE SYMMETRY OF THE ORDER PARAMETER AND FOR A DEVELOPMENT OF CONCEPTS FOR QUBITS

The particular junction configurations investigated in this work allow some consideration of the possible impact of these types of junctions on the study of the Josephson effect and the order parameter symmetry in YBCO and on the development of concepts for devices.[1,6,9,7] We first recall that the biepitaxial technique can provide circuits composed completely of junctions without any π-loops (see Fig. 9a). By varying the interface orientation with respect to the [103] electrode orientation, the junction properties can be adjusted. On the other hand the traditional biepitaxial technique,[11] producing 45° [001] tilt GBs (see Fig. 9b) or the types of junctions described in the previous section by using CeO_2 (see Fig. 9c), can controllably generate π-loops on macroscopic scales. In these schemes we use a corner geometry with a 90° angle. This angle α can be obviously tuned to enhance the effects related to the phase shift (see dashed line in Fig.9b) and this change is particularly easy to realize by using the biepitaxial technique.

In this section we focus our attention mainly on the feasibility of the biepitaxial junctions to obtain the doubly degenerate state required for a qubit. In Ref.[1a] the design is based on quenching the lowest order coupling by arranging a junction with its normal aligned with the node of the d-wave order parameter, thus producing a double periodic current-phase relation. It has been shown that the use of π phase shifts in a superconducting phase qubit provides a naturally bistable device and does not require external bias currents and magnetic fields.[1b] The direct consequence is the quietness of the device over other designs. A π junction provides the required doubly degenerate fundamental state, which also manifests itself in a doubly periodic function of the critical current density as a function of the phase.[8] The same principle has been used in small inductance five junction loop frustrated by a π-phase shift.[1b] This design provides a perfectly degenerate two-level system and offers some advantages in terms of fabrication ease and performance. HTS may represent a natural solution for the realization of the required π-phase shift due to the pairing symmetry of the order parameter and, therefore, due to the possibility of producing π phase shifts. Experimental evidence of YBCO π -SQUIDs has been given by employing the bicrystal technique on special tetracrystal substrates.[7] The biepitaxial technique, beyond providing junctions with opportune properties, would guarantee the versatility necessary for the implementation of a real device, as shown below. As a matter of fact, we notice that our technique allows the realization of circuits where π-loops can be controllably located in part of the substrate and separated from the rest of the circuit based on "0"-loops, i.e. junctions where no additional π phase shifts arise. This can be easily made by depositing the MgO and CeO_2 seed layers on different parts of the substrate, which will be also partly not covered by any seed layer.

As a test to show how the biepitaxial junctions could be considered for preliminary tests and device implementation for quantum computing without the topological restriction imposed by the bicrystal technique, we refer to the structures proposed in Ref.[1]as exemplary circuits.

The former is composed by a s-wave (S)- d-wave (D)- s-wave (S') double junction connected with a capacitor and an ordinary "0" Josephson junction based on s-wave superconductors (the S-D'-S junction generates the doubly degenerate state). The latter consists of a five junction loop with a π junction. Our technique would combine the possibility of placing the ordinary "0" junctions corresponding to the MgO seed layer and to exploit the possible doubly degenerate state of asymmetric 45° GB junctions corresponding to the CeO_2 seed layer to replace the S-D-S' system or the π junction respectively. Our structure would be obviously composed only of HTS. In Figs. 10a and 10b we show how devices for instance such as those proposed in Ref.[1] could be obtained by employing the biepitaxial technique respectively. The application to the five junction loop is straightforward (Fig.10b) and the advantages of this structure have been already discussed in Ref.[1b]. The biepitaxial technique can offer possible alternatives for the realization of the structures above. In particular the double junctions of the original S-D-S' system can be also replaced by a D'-D-D" structure (Fig.10c) by exploiting our technique, in contrast to the bicrystal technology which could not give this possibility. Such a configuration could offer some advantages, if we consider that asymmetric 45° bicrystal GB Josephson junctions did not give systematic evidence of the doubly degenerate state. The doubly degenerate state seems to occur only in high quality low transparency GB junctions[8,26] and it is known that S-I-D junctions do not have double periodicity of the critical current as a function of the phase.[26] A consequence of a possible nodeless order parameter[4,23] at the D-D' GB interface could be a closer similarity with a S-I-D junction with loss of the doubly degenerate state. If this is the case, we speculate that the double junctions structure for symmetry reasons would produce a leading term in the Josephson coupling energy of the form $E_d \cos 2\theta$ (double periodic) and that the possible dipolar component of the magnetic field would be almost completely compensated in this configuration.[1b] This can be considered as an attempt to construct a "microscopic" 2θ-junction. We finally notice that the topological advantages offered by the biepitaxial junctions would therefore be crucial in both the cases considered for the realization of the structure in Fig. 10, and important to reduce de-coherence effects. Bicrystal substrates would in fact impose on the circuit additional junctions required by the circuit design and, as a consequence, generate additional noise and de-coherence in the device.

V. CONCLUSIONS

The performance of the presented junctions and SQUIDs demonstrates that significant improvements in the biepitaxial technique are possible, and the resulting devices have potential for applications. We have presented a phenomenology that is consistent with the expected absence of π-loops in 45° [100] tilt and twist grain boundaries junctions. The use of a CeO_2 rather than a MgO seed layer can produce π-loops in the same junction configurations. The versatility of the biepitaxial technique has been recently used to obtain different types of grain boundaries. The advantage of placing junctions in arbitrary locations on the substrate without imposing any restrictions on the geometry, and the ease of obtaining different device configurations by suitably patterning the seed layer, make the biepitaxial technique competitive for the testing of new concept devices, such as those based on π-loops. Some simple examples of situations in which π-loops can be suitably produced in specific locations of a more complicated circuit have also been discussed.

ACKNOWLEDGMENTS

This work has been partially supported by the projects PRA-INFM "HTS Devices" and SUD-INFM "Analisi non distruttive con correnti parassite tramite dispositivi superconduttori" and by a MURST COFIN98 program (Italy). The authors would like to thank Dr. E. Ilichev and A. Golubov for interesting discussions on the topic.

---

[1] L.B. Ioffe, V.B. Geshkenbein, M.V. Feigel'man, A.L. Fauchere and G. Blatter, Nature **398**, 679 (1999); G. Blatter, V. B. Geshkenbein and L. B. Ioffe, Cond. Mat. 9912163 (1999)

[2] L.N. Bulaevskii, V.V. Kuzii and A.A. Sobyanin, JETP Lett. **25**, 290 (1977)

[3] V.B. Geshkenbein, A.I. Larkin and A. Barone, Phys. Rev. B **36**, 235 (1986)

[4] C.C. Tsuei and J.R. Kirtley, to be published in Review of Modern Physics (1999); C.C. Tsuei, J.R. Kirtley, C.C. Chi, L.S. Yu-Jahnes, A. Gupta, T. Shaw, J.Z. Sun and M.B. Ketchen, Phys. Rev. Lett. **73**, 593 (1994); J.R. Kirtley, C.C. Tsuei, J.Z. Sun, C.C. Chi, L.S. Yu-Jahnes, A. Gupta, M. Rupp and M.B. Ketchen, Nature **373**, 225 (1995); D.A. Wollman, D.J. Van Harlingen, J. Giapintzakis, D.M. Ginsberg, Phys. Rev. Lett. 74, 797 (1995); D.A. Wollman, D.J. Van Harlingen and A.J. Leggett, Phys. Rev. Lett. 73, 1872 (1994)

[5] M. Sigrist and T.M. Rice, J. Phys. Soc. Jap.**61**, 4283 (1992)

[6] A.M. Zagoskin, Cond. Mat. 9903170 (1999)

[7] R. Schulz, B. Chesca, B. Goetz, C.W. Schneider, A. Shmehl, H. Bielefeldt, H. Hilgenkamp and J. Mannhart, Appl. Phys. Lett.**76**, 912 (2000)

[8] E. Il'ichev, V. Zakosarenko, R.P.J. Ijsselsteijn, H.E. Honig, V. Schultze, H.G. Meyer, M. Grajcar and R. Hlubina, Phys. Rev. B **60**, 3096 (1999)

[9] E. Terzioglu and M.R. Beasley, IEEE Trans. Appl. Supercond. **8**, 48 (1998)

[10] F. Tafuri, F. Miletto Granozio, F. Carillo, A. Di Chiara, K. Verbist and G. Van Tendeloo, Phys. Rev. B **59**, 11523 (1999)

[11] K. Char, M.S. Colclough, S.M. Garrison, N. Newman and G. Zaharchuk, Appl. Phys. Lett. **59**, 773 (1991)

[12] D. Dimos, P. Chaudari, J. Mannhart and F.K. LeGoues, Phys. Rev. Lett. **61**, 219 (1988)

[13] R. W. Simon, J.F. Burch, K.P. Daly, W.D. Dozier, R. Hu, A.E. Lee, J.A. Luine, H.M. Manasevit , C.E. Platt, S.M. Schwarzbek, D.St. John, M.S. Wire and M.J. Zani, in "Science and Technology of Thin Films Superconductors 2", R.D. McConnel and R. Noufi Eds.(Plenum, New York, 1990), p. 549

[14] J. Mannhart, H. Hilgenkamp, B. Mayer, Ch. Gerber, J.R. Kirtley, K.A. Moler and M. Sigrist, Phys. Rev. Lett. **77**, 2782 (1996)

[15] U. Scotti di Uccio, F. Lombardi, F. Ricci, E. Manzillo, F. Miletto Granozio, F. Carillo and F. Tafuri unpublished (2000)

[16] K. Verbist , O. Lebedev, G. Van Tendeloo, F. Tafuri, F. Miletto Granozio and A. Di Chiara, Appl. Phys. Lett. **74**, 1024 (1999)

[17] A. Barone and G. Paternoò, Physics and Applications of the Josephson Effect, (J. Wiley, New York, 1982)

[18] J. Mannhart, R. Gross, K. Hipler, R.P. Huebner, C.C. Tsuei, D. Dimos and P. Chaudari, Science **245**, 839 (1989)

[19] F. Tafuri, B. Nadgorny, S. Shokhor, M. Gurvitch, F. Lombardi, F. Carillo, A. Di Chiara and E. Sarnelli, Phys. Rev. B **57**, R14076 (1998)

[20] F. Tafuri, S. Shokhor, B. Nadgorny, M. Gurvitch, F. Lombardi and A. Di Chiara, Appl. Phys. Lett. **71**, 125 (1997)

[21] J.R. Kirtley *et al.*, *Appl. Phys. Lett.* **66**, 1138 (1995)

[22] F. Tafuri and J.R. Kirtley, cond-mat /0003106.

[23] D.B. Bailey, M. Sigrist and R.B. Laughlin, Phys. Rev. B **55**, 15239 (1997);M. Sigrist, Progr. Theor. Physics *99*, 899 (1998).

[24] G. Testa, E. Sarnelli, F. Carillo and F. Tafuri, Appl. Phys. Lett. **75**, 3542 (1999)

[25] A.H. Miklich, J. Clarke, M.S. Colclough, and K. Char, Appl. Phys. Lett. **60**, 1989 (1992)

[26] Y. Tanaka and S. Kashiwaya, Phys. Rev. B **56**, 893 (1997)

FIG. 1. A schematic representation of the artificial grain boundary structure. The boundary is obtained at the interface between the [001] oriented YBCO film grown on the [110] MgO seed layer and the [103] YBCO film grown on the bare [110] STO substrate. In contrast with the 45° [001] tilt bicrystal junctions, in this case the order parameter orientations do not produce an additional π phase shift.

FIG. 2. The CeO_2 seed layer produces an artificial GB that can be seen as a result of two rotations: a 45° [100] tilt or twist followed by a 45° tilt around the c-axis of the (001) film. For this junction configuration a d-wave order parameter symmetry would produce π -loops.

FIG. 3. Current vs voltage (I-V) characteristics of the biepitaxial junction for temperature close to the critical temperature. In the inset the I-V curve at T = 4.2 K is shown.

FIG. 4. a) Scheme of the seed layer patterning,which allows the measuremment on the same chip of the properties of a tilt junction and of junctions whose interface is tilted in plane of an angle $\alpha = 30°, 45°$ and 60° with respect the a- or b-axis of the (001) YBCO thin film respectively. b) The I-V characteristics (measured at T = 4.2 K) of the microbridges reported in Fig. 4a.

FIG. 5. Magnetic-field dependence of the critical current of a [100] tilt biepitaxial dc-SQUID. The absolute maximum is observed for zero field. A double-period modulation is observed.The longer period modulation is the diffraction pattern due to the magnetic field sensed by a single junction, while the shorter period SQUID modulation is shown more clearly in the inset (a). In the inset (b) I-V curves are shown as a function of an externally applied magnetic field at T = 4.2 K. A typical Fraunhofer-like dependence is evident.

FIG. 6. Scanning SQUID microscope image of a 200x200μm^2 area along a grain boundary separating a (100) region from a (103) region of a thin YBCO biepitaxial film grown. The position of the grain boundary is indicated by the dashed line.

FIG. 7. Magnetic field dependence of the voltage of a [100] tilt biepitaxial dc-SQUID at 77 K for different values of the bias current.

FIG. 8. Magnetic flux noise spectral densities of a [100] tilt biepitaxial SQUID at T=77 K and T=4.2 K. The SQUID, with an inductance L=13 pH, was modulated with a standard flux-locked-loop electronics. The right axis shows the energy resolution. Data at T = 4.2 K are compared with results on SQUIDs based on [001] tilt biepitaxial junctions from Ref. 25.

FIG. 9. a) 3-dimensional view of a SQUID based on 45° [100] tilt and twist GBs; no π-loops should occur. b) Top view of π-SQUID based on 45° [001] tilt GBs. c) 3-dimensional view of a π-SQUID based on GBs resulting from two rotations: a 45° [100] tilt or twist followed by a 45° [001] tilt

FIG. 10. Scheme of the qubit structure proposed in Ref.1 designed using the biepitaxial grain boundaries proposed in the paper. The double junctions of the original S-D-S' system can be also replaced by D'-D-D".

Anomalous Periodicity of the Current-Phase Relationship of Grain-Boundary Josephson Junctions in High-T_c Superconductors

E. Il'ichev, V. Zakosarenko, R.P.J. IJsselsteijn, H. E. Hoenig, V. Schultze, H.-G. Meyer
Department of Cryoelectronics, Institute for Physical High Technology, P.O. Box 100239, D-07702 Jena, Germany

M. Grajcar and R. Hlubina
Department of Solid State Physics, Comenius University, Mlynská Dolina F2, 842 15 Bratislava, Slovakia

(December 14, 2002)

The current-phase relation (CPR) for asymmetric 45° Josephson junctions between two d-wave superconductors has been predicted to exhibit an anomalous periodicity. We have used the single-junction interferometer to investigate the CPR for this kind of junctions in $YBa_2Cu_3O_{7-x}$ thin films. Half-fluxon periodicity has been experimentally found, providing a novel source of evidence for the d-wave symmetry of the pairing state of the cuprates.

There is growing evidence in favor of the $d_{x^2-y^2}$-wave symmetry of the pairing state of the high-temperature superconductors.[1] An unconventional pairing state requires the existence of zeros of the order parameter in certain directions in momentum space. Thermodynamic and spectroscopic measurements do indeed suggest their existence, but by themselves they do not exclude conventional s-wave pairing with nodes.[1] Direct evidence for the d-wave pairing state is provided by phase-sensitive experiments, which are based on the Josephson effect.[2] Quite generally, the current-phase relationship (CPR) of a Josephson junction, $I(\varphi)$, is an odd periodic function of φ with a period 2π.[3] Therefore $I(\varphi)$ can be expanded in a Fourier series

$$I(\varphi) = I_1 \sin\varphi + I_2 \sin 2\varphi + \ldots . \qquad (1)$$

In the tunnel limit we can restrict ourselves to the first two terms in Eq. (1). Since the order parameter is bound to the crystal lattice, $I(\varphi)$ of a weak link depends on the orientation of the d-wave electrodes with respect to their boundary. The existing phase-sensitive experiments exploit possible sign changes of I_1 between different geometries.[2] In this Letter we present a new phase-sensitive experimental test of the symmetry of the pairing state of the cuprates. Namely, in certain geometries, the I_1 term should vanish by symmetry. In such cases, the CPR should exhibit an anomalous periodicity.

Let us analyze the angular dependence of $I_{1,2}$ in a junction between two macroscopically tetragonal d-wave superconductors. As emphasized in Ref. 4, also heavily twinned orthorhombic materials such as $YBa_2Cu_3O_{7-x}$ belong to this class, if the twin boundaries have odd symmetry. We consider first an ideally flat interface between the superconducting electrodes. Let θ_1 (θ_2) denote the angle between the normal to the grain boundary and the a axis in the electrode 1 (2), see Fig. 1. If we keep only the lowest-order angular harmonics, the symmetry of the problem dictates that[4]

$$I_1 = I_c \cos 2\theta_1 \cos 2\theta_2 + I_s \sin 2\theta_1 \sin 2\theta_2 . \qquad (2)$$

The coefficients I_c, I_s are functions of the barrier strength, temperature T, etc. The I_2 term results from higher-order tunneling processes and we neglect its weak angular dependence. It is seen from Eq. (2) that the criterion for the observation of an anomalous CPR, $I_1 = 0$, is realized for an asymmetric 45° junction, i.e. a junction with $\theta_1 = 45°$ and $\theta_2 = 0$. For an interface which is not ideally flat, $\theta_i = \theta_i(x)$ are functions of the coordinate x along the junction. $I_1 = 0$ remains valid even in this case, if the average values $\langle\theta_1(x)\rangle = 45°$ and $\langle\theta_2(x)\rangle = 0$.

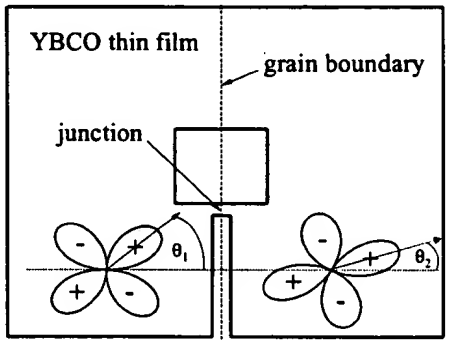

FIG. 1. Sketch of the interferometer (not in scale).

The I_2 term is present also in weak links based on conventional s-wave superconductors but for all known types of weak links $|I_2/I_1| < 1$. For instance, for a tunnel junction $|I_2/I_1| \ll 1$. For a SNS junction, $I \propto \sin\varphi/2$ at $T = 0$,[5] and the Fourier expansion Eq. (1) leads to $I_2/I_1 = -2/5$. Therefore, a possible experimental observation of $|I_2/I_1| \gg 1$ in an asymmetric 45° junction provides direct evidence of d-wave symmetry of the pairing state in the cuprates.

We have investigated the CPR of $YBa_2Cu_3O_{7-x}$ thin film bicrystals with asymmetric 45° [001]-tilt grain boundaries[6–8] as sketched in Fig. 1, using a single-junction interferometer configuration in which the

Josephson junction is inserted into a superconducting loop with a small inductance L. In a stationary state without fluctuations, the phase difference φ across the junction is controlled by applying external magnetic flux Φ_e penetrating the loop: $\varphi = \varphi_e - \beta f(\varphi)$. Here $\varphi_e = 2\pi\Phi_e/\Phi_0$ is the external flux normalized to the flux quantum $\Phi_0 = 2.07 \times 10^{-15}$ Tm^2. The CPR is written as $I(\varphi) = I_0 f(\varphi)$, where I_0 is the maximal Josephson current. $\beta = 2\pi L I_0/\Phi_0$ is the normalized critical current. In order to obtain the CPR for the complete phase range $-\pi \leq \varphi \leq \pi$ the condition $\beta < 1$ has to be fulfilled, because for $\beta > 1$ the curve $\varphi(\varphi_e)$ becomes multivalued and there are jumps of φ and a hysteresis for a sweep of φ_e. Following Ref. 3, we express the effective inductance of the interferometer using the derivative f' with respect to φ as $L_{int} = L[1+1/f'(\varphi)]$. The inductance can be probed by coupling the interferometer to a tank circuit with inductance L_T, quality factor Q, and resonance frequency ω_0.[9] External flux in the interferometer is produced by a current $I_{dc} + I_{rf}$ in the tank coil and can be expressed as $\varphi_e = 2\pi(I_{dc}+I_{rf})M/\Phi_0 = \varphi_{dc}+\varphi_{rf}$, where $M^2 = k^2 L L_T$, and k is a coupling coefficient. Taking into account the quasiparticle current in the presence of voltage V across the junction the phase difference is given by the relation $\varphi = \varphi_{dc} + \varphi_{rf} - \beta f(\varphi) - 2\pi\tau(\varphi)V/\Phi_0$, where $\tau(\varphi) = L/R_J(\varphi)$ and $R_J(\varphi)$ is the resistance of the junction . In the small-signal limit $\varphi_{rf} \ll 1$ and in the adiabatic case $\omega\tau \ll 1$, keeping only the first-order terms, the effective inductance L_{eff} of the tank curcuit-interferometer system reads

$$L_{eff} = L_T\left(1 - k^2\frac{L}{L_{int}}\right) = L_T\left(1 - \frac{k^2\beta f'(\varphi)}{1+\beta f'(\varphi)}\right).$$

Thus the phase angle α between the driving current and the tank voltage U at the resonant frequency of the tank circuit ω_0 is

$$\tan\alpha(\varphi) = \frac{k^2 Q\beta f'(\varphi)}{1+\beta f'(\varphi)}. \qquad (3)$$

Using the relation $[1+\beta f'(\varphi)]d\varphi = d\varphi_{dc}$ valid for $\varphi_{rf} \ll 1$ and $\omega\tau \ll 1$, one can find the CPR from Eq. (3) by numerical integration.

The advantage of the measurement of the CPR of an asymmetric 45° junction with respect to the by-now standard phase-sensitive tests of pairing symmetry based on the angular dependence of I_1 is twofold. First, it avoids the complications of the analysis of experiments caused by the presence of the term I_s.[4] Second, a flux trapped in the SQUID does not invalidate the conclusions about the ratio $|I_2/I_1|$ and hence about the pairing symmetry, while this is not the case in standard phase-sensitive tests of the d-wave symmetry of the pairing state.[10]

The films of thickness 100 nm were fabricated using standard pulsed laser deposition on (001) oriented $SrTiO_3$ bicrystalline substrates with asymmetric [001] tilt misorientation angles 45° ± 1°. They were subsequently patterned by Ar ion-beam etching into 4×4 mm^2 square washer single-junction interferometer structures (Fig. 1). The widths of the junctions were $1 \div 2$ μm. The washer square holes had a side-length of 50 μm. This geometry of the interferometer gives $L \approx 80$ pH. The resistance of the junction is higher than 1 Ω and the condition for the adiabatic limit $\omega\tau \ll 1$ is satisfied. For measurements of $\alpha(\varphi_{dc})$, several tank circuits with inductances $0.2 \div 0.8$ μH and resonance frequencies $16 \div 35$ MHz have been used. The unloaded quality factor of the tank circuits $70 < Q < 150$ has been measured at various temperatures. The coupling factor k was determined from the period ΔI_{dc} of $\alpha(I_{dc})$ using $M\Delta I_{dc} = \Phi_0$. Its value varied between 0.03 and 0.09. The amplitude of I_{rf} was set to produce the flux in the interferometer lower than $0.1\Phi_0$.

The measurements have been performed in a gas-flow cryostat with a five-layer magnetic shielding in the temperature range $4.2 \leq T < 90$ K. The experimental setup was calibrated by measuring interferometers of the same size with 24° and 36° grain boundaries. We have studied 5 samples, out of which sample No. 1 exhibited the most anomalous behavior. Samples Nos. 2,3 were less anomalous and the remaining two samples had high critical currents and their $I(\varphi)$ was conventional. In Fig. 2 we plot the phase angle α as a function of the dc current I_{dc} for samples Nos. 1,2. The data for the 36° junction is shown for comparison. Note that at $T = 40$ K the periodicity of $\alpha(I_{dc})$ is the same for all samples.

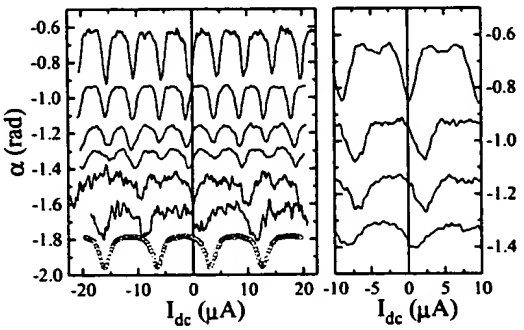

FIG. 2. Left panel: Phase angle between the driving current and the output voltage measured for the sample No. 1 at different temperatures as a function of the dc current I_{dc}. The curves are shifted along the y axis and the data for $T = 30$ and 40 K are multiplied by factor 4 for clarity. From top to bottom, the data correspond to T =4.2, 10, 15, 20, 30 and 40 K. The data measured on 36° bicrystals ($\theta_1 \approx 36°, \theta_2 \approx 0$) at T =40 K in the same washer geometry are shown for comparison (open circles). Right panel: The same for the sample No. 2. From top to bottom, the data correspond to T =4.2, 10, 15 and 20 K.

We assume that the period of $\alpha(I_{dc})$ at T =40 K, ΔI_{dc} =9.6 μA, corresponds to $\Delta\varphi_{dc} = 2\pi$. In order to determine the CPR we take $\varphi_{dc} = 0$ at a maximum or minimum of α. This is necessary in order to satisfy

$I(\varphi = 0) = 0$, as required by general principles.[3] The experimentally observed shift of the first local extreme of $\alpha(I_{dc})$ from $I_{dc} = 0$ (Fig. 2) can be due to flux trapped in the interferometer washer. Most probably, this flux resides in the long junction of the interferometer. The long junction does not play an active role because the Josephson penetration depth is much shorter than its length, and external fields producing I_{dc} are smaller than its critical field. Nevertheless the long junction sets the phase difference for $I_{dc} = 0$ at the small junction.

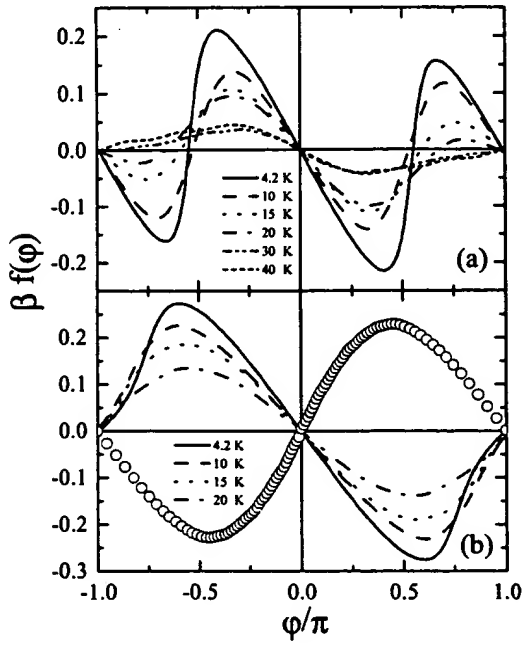

FIG. 3. a) Josephson current through the junction for the sample No. 1 as a function of the phase difference φ, determined from the data in Fig. 2. The statistics of $\alpha(\varphi)$ was improved by folding the data back to the interval $\langle 0, \pi \rangle$ and taking an average. The symmetry $\alpha(\varphi) = \alpha(-\varphi)$ was assumed. b) The same for the sample No. 2. The data for the asymmetric 36° bicrystal at $T = 40$ K (open circles) is also shown.

In Fig. 3, we show the CPR determined from the data in Fig. 2. For all curves we have performed a minimal necessary shift consistent with $I(\varphi = 0) = 0$. Thus, for the samples Nos. 1,2 we have assumed that at $\varphi_{dc} = 0$ a minimum of $\alpha(\varphi_{dc})$ is realized. For an interferometer with a conventional s-wave weak link (and also for the 36° junction), at $\varphi_{dc} = 0$ a maximum of $\alpha(\varphi_{dc})$ is realized. Note that the maximum (minimum) of $\alpha(\varphi_{dc})$ at $\varphi_{dc} = 0$ implies a diamagnetic (paramagnetic) response of the interferometer in the limit of small applied fields. In Fig. 4 we plot the coefficients I_1 and I_2 determined by Fourier analysis of the CPR for the sample No. 1 at various temperatures. With decreasing T, $|I_2|$ grows monotonically down to $T = 4.2$ K, while the I_1 component exhibits only a weak temperature dependence.

Our experimental results can be understood as follows. Deviations from ideal geometry of the asymmetric 45° junction, $\langle \theta_1 \rangle = 45° + \alpha_1$ and $\langle \theta_2 \rangle = \alpha_2$, lead to a finite value of I_1. Thus, imperfections of the junction increase its critical current. For this reason we believe that samples Nos. 2-5 contain imperfections and from now we concentrate on nearly ideal junctions (such as sample No. 1) with $|\alpha_1|, |\alpha_2| \ll 1$. For such junctions, the ratio I_2/I_1 exhibits the following temperature dependence. For $T \to 0$, $|I_2/I_1| \gg 1$. The region $T \sim T_c$ can be analyzed quite generally within Ginzburg-Landau theory. Let the electrodes be described by (macroscopic) order parameters $\Delta_{1,2} = |\Delta| e^{i\varphi_{1,2}}$. Then the phase-dependent part of the energy of the junction is $E = a[\Delta_1 \Delta_2^* + \text{H.C.}] + b[(\Delta_1 \Delta_2^*)^2 + \text{H.C.}] + \ldots$ where $a, b, \ldots$ depend weakly on T.[11] Thus for T close to T_c we estimate $I_1 \propto |\Delta|^2 \propto (T_c - T)$ and $I_2 \propto |\Delta|^4 \propto (T_c - T)^2$, leading to $|I_2/I_1| \ll 1$. These expectations are qualitatively consistent with the experimental data shown in Fig. 4.

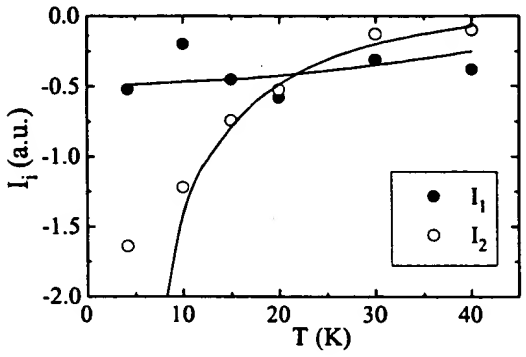

FIG. 4. Temperature dependence of the Fourier expansion coefficients $I_{1,2}$ determined from the experimental data in Fig. 3a. Solid lines are the Fourier expansion coefficients for the numerical data in Fig. 5.

So far, our discussion was based solely on symmetry arguments. Let us attempt a more quantitative analysis of our data now. Two different microscopic pictures of asymmetric 45° Josephson junctions between d-wave superconductors have been considered in the literature. The first picture assumes a microscopically tetragonal material and an ideally flat interface.[11–13] Within this picture, there are two contributions to the Josephson current. The first is due to bulk states and in the tunnel limit it is well described by the Sigrist-Rice term I_c in Eq. (2).[14] The second is due to mid-gap states which develop close to the surfaces of unconventional superconductors.[15] $I(\varphi)$ for the sample No. 1 calculated according to the model of Ref. 12 is shown in Fig. 5. The experimental data can be fitted by a relatively broad range of barrier heights. However, if we require the 36° junction to be fitted by the same (or smaller) barrier height as for the 45° junction, we conclude the barrier must be rather low.[16] The T dependence of $I(\varphi)$ requires

a choice of $T_c \approx 60$ K in the non-selfconsistent theory of Ref. 12. The reduction from the bulk $T_c = 90$ K is probably due to a combined effect of surface degradation and order-parameter suppression at the sample surface. The temperature dependence of the ratio of the π and 2π periodic components in $I(\varphi)$ is seen to be in qualitative agreement with experimental data in Fig. 3a. This is explicitly demonstrated in Fig. 4 where we compare the experimentally obtained $I_{1,2}$ with the results of the Fourier analysis of the curves in Fig. 5. The divergence of I_2 as $T \to 0$ is an artifact of the ideal junction geometry assumed in Ref. 12. If the finite roughness of the interface is taken into account, this divergence is cut off and the experimental data in Fig. 4 do indeed resemble theoretical predictions for a rough interface.[13] However, the nonselfconsistent theory of Ref. 12 is unable to explain the experimentally observed steep CPR close to the minima of the junction energy (see Fig. 3a). In the limit of vanishing barrier height, the theoretical CPR does have steep portions, but these are located close to the maxima of the junction energy (see also Ref. 11).

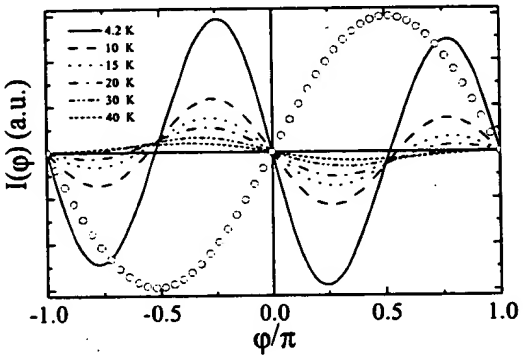

FIG. 5. $I(\varphi)$ calculated according to Eq. (64) of Ref. 12 for a junction with $\theta_1 = 45.5°$, $\theta_2 = 0$, $\lambda d = 1.5$, $\kappa = 0.5$, and $T_c = 60$ K. $I(\varphi)$ at $T = 40$ K for the 36° bicrystal (open circles) was calculated for the same parameters except for $\theta_1 = 36°$.

In a different approach to the asymmetric 45° junction, one assumes a heavily twinned orthorhombic material (which is macroscopically tetragonal, however) and/or a meandering interface with $\theta_i = \theta_i(x)$.[17,18] Hence the critical current density $j_c(x)$ is a random function with a typical amplitude $\langle |j_c(x)| \rangle \sim j_c$. If the average critical current along the junction $\langle j_c \rangle \ll j_c$, a spontaneous flux is generated in the junction, and $|I_2/I_1| \gg 1$.[17,18] In particular, for $\langle \theta_1 \rangle = 45°$ and $\langle \theta_2 \rangle = 0$, there is an equal amount of parts having positive and negative j_c, leading to $\langle j_c \rangle = 0$ and $I_1 = 0$. Note that also within the picture of Refs. 17,18, the d-wave symmetry of the pairing state is crucial, otherwise the condition $\langle j_c \rangle \ll j_c$ is difficult to satisfy.

Our present understanding of $I(\varphi)$ in the asymmetric 45° junction is only qualitative. There is considerable experimental evidence[6–8] that the grain boundary junctions are at most piecewise flat. However, we cannot say whether the shape of $I(\varphi)$ is dominated by the mid-gap states in the microscopically flat regions, or by spontaneous flux generation due to the spatial inhomogeneity of the junction. This issue requires further study.

In conclusion, we have measured the magnetic field response of a single-junction interferometer based on asymmetric 45° grain-boundary junctions in $YBa_2Cu_3O_{7-x}$ thin films. Half-fluxon periodicity has been experimentally found, in agreement with theoretical predictions for $d_{x^2-y^2}$-wave superconductors. Hence, our results provide a novel source of evidence for the d-wave symmetry of the pairing state in the cuprates.

Financial support by the DFG (Ho 461/1-1) is gratefully acknowledged. M. G. and R. H. were supported by the Slovak Grant Agency Grant No. 1/4300/97 and the Comenius University Grant No. UK/3927/98.

[1] For a review, see J. Annett, N. Goldenfeld, and A. J. Leggett, in *Physical Properties of High Temperature Superconductors*, edited by D. M. Ginsberg (World Scientific, New Jersey, 1996), Vol. V.
[2] See C. C. Tsuei *et al.*, Science **271**, 329 (1996) and references therein.
[3] A. Barone and G. Paterno, *Physics and Applications of the Josephson Effect*, (Wiley, New York, 1982).
[4] M. B. Walker and J. Luettmer-Strathmann, Phys. Rev. B **54**, 588 (1996).
[5] I. O. Kulik and A. N. Omel'yanchuk, Fiz. Nizk. Temp. **4**, 296 (1978) [Sov. J. Low Temp. Phys. **4**, 142 (1978)].
[6] J. R. Kirtley *et al.*, Phys. Rev. B **51**, 12 057 (1995).
[7] H. Hilgenkamp, J. Mannhart, and B. Mayer, Phys. Rev. B 53, 14586 (1996).
[8] J. Mannhart *et al.*, Phys. Rev. Lett. **77**, 2782 (1996).
[9] E.V. Il'ichev *et al.*, J. Low Temp. Phys. **106**, 503 (1997).
[10] R. A. Klemm, Phys. Rev. Lett. **73**, 1871 (1994).
[11] A. Huck, A. van Otterlo, and M. Sigrist, Phys. Rev. B **56**, 14 163 (1997).
[12] Y. Tanaka and S. Kashiwaya, Phys. Rev. B **56**, 892 (1997).
[13] Y. S. Barash, H. Burkhardt, and D. Rainer, Phys. Rev. Lett. **77**, 4070 (1996).
[14] M. Sigrist and T. M. Rice, J. Phys. Soc. Jpn. **61**, 4293 (1992).
[15] C. R. Hu, Phys. Rev. Lett. **72**, 1526 (1994).
[16] This is consistent with the Fourier analysis of the data in Fig. 3 which finds non-negligible I_n also for $n \geq 3$.
[17] A. J. Millis, Phys. Rev. B **49**, 15 408 (1994).
[18] R. G. Mints, Phys. Rev. B **57**, R322 (1998).

Bi-epitaxial grain boundary junctions in $YBa_2Cu_3O_7$

K. Char, M. S. Colclough, S. M. Garrison, N. Newman, and G. Zaharchuk
Conductus, Inc., Sunnyvale, California 94086

(Received 26 March 1991; accepted for publication 13 May 1991)

We have developed a new way of making grain boundary junctions in $YBa_2Cu_3O_7$ thin films by controlling the in-plane epitaxy of the deposited film using seed and buffer layers. We produce 45° grain boundaries along photolithographically defined lines. The typical value of the critical current density of the junctions is 10^3–10^4 A/cm^2 at 4.2 K and 10^2–10^3 A/cm^2 at 77 K, while the rest of the film has a critical current density of 1–3×10^6 A/cm^2 at 77 K. The current-voltage characteristics of the junctions show resistively shunted junction behavior and we have used them to fabricate dc superconducting quantum interference devices (SQUIDs) which show modulation at temperatures well above 77 K. This is the first planar high T_c Josephson junction technology that appears readily extendable to high T_c integrated circuits.

Most microelectronic applications of the high T_c superconductors will rely upon microbridges such as superconductor-normal metal-superconductor (S-N-S) junctions or other weak link geometries instead of superconductor-insulator-superconductor (S-I-S) tunnel junctions. A number of weak-link structures provide reliable critical current reduction in $YBa_2Cu_3O_7$ (YBCO) thin films; grain boundary junctions.[1–3] traditional edge junctions,[4] microbridges grown across a sharp substrate step,[5] and S-N-S-type junctions with Au,[6] $PrBa_2Cu_3O_7$,[7,8] or $SrTi_{1-x}Nb_xO_3$ (Ref. 9) normal layers. Of these various weak-link geometries, grain boundary junctions work well at temperatures close to T_c, have reasonably high I_cR_n products, and show behavior explained by a resistively shunted junction model with a relatively uniform current density. To date, the high angle grain boundary junctions that have been used were formed either by fusing differently oriented $SrTiO_3$ substrates[1] or by patterning the randomly occurring grain boundaries in granular films.[2,3] Superconducting quantum interference devices (SQUIDs) made from the grain boundaries on $SrTiO_3$ bicrystals had reasonable signal and low noise[10] up to temperatures very close to the T_c of the film. However, this $SrTiO_3$ bicrystal technique has a major drawback: it cannot be readily extended to integrated circuits. On the other hand, SQUIDs made from granular films are plagued by low yield and the presence of grain boundaries in the SQUID loop itself. These lead to excessive flux noise and hysteresis in the voltage-flux response of the SQUID.

In this letter, we report for the first time the successful fabrication of high T_c weak-link Josephson junctions operating at and above 77 K that are made from grain boundary junctions whose locations are determined by conventional photolithography. This result demonstrates the feasibility of an extendable technology for fabricating high T_c Josephson devices which avoids the problems associated with the devices made from granular thin films and on bicrystal substrates. We reproducibly fabricate 45° grain boundaries in YBCO films by controlling their in-plane epitaxy using seed and buffer layers deposited on *r*-plane sapphire substrates, a method we call "bi-epitaxy." The method is quite general, and can be used on a wide variety of substrates.

Recently, we reported[11] the existence of two in-plane epitaxial orientations of *c*-axis oriented epitaxial YBCO thin films on yttria-stabilized zirconia (YSZ), resulting from the poor lattice match between YBCO and YSZ. This observation led us to realize that it would be possible to make bi-epitaxial grain boundaries on such a substrate using seed and buffer layers, or, in an alternative geometry, on a well lattice-matched substrate using poorly lattice-matched seed layers. For example, we previously reported[12] the growth of YBCO thin films on *r*-plane sapphire using buffer layers such as $SrTiO_3$, $CaTiO_3$, YSZ, and MgO. We emphasized the importance of the in-plane epitaxy of YBCO, particularly because high-angle grain boundaries in YBCO films behave as weak links, leading to low critical current densities and high surface resistances.[12,13] Our efforts towards minimizing the occurrence of these high-angle grain boundaries taught us how to control them and led us to design and demonstrate a variety of 45° weak-link junctions. One example takes advantage of the differing epitaxial directions of two different layers, MgO and $SrTiO_3$, when they are deposited on an *r*-plane sapphire substrate. Using these two layers as a seed and a buffer layer, we have succeeded in fabricating bi-epitaxial 45° grain boundaries in YBCO on sapphire substrates by the following process.

Schematic views of our device structure are shown in Fig. 1. We first deposit 3–30 nm of epitaxial MgO as a seed layer on an *r*-plane sapphire substrate. MgO is produced by laser ablating a Mg metallic target in a 2–20 mTorr oxygen atmosphere with a substrate temperature of 300–700 °C. We then mask the MgO with conventional photoresist and remove it from, for example, half of the substrate by either Ar ion beam milling or chemical wet etching with dilute phosphoric acid. We then grow 10–100 nm of epitaxial $SrTiO_3$ buffer layer by laser ablation on both the exposed sapphire surface and on the patterned MgO seed layer. The deposition conditions are an oxygen pressure of 100–200 mTorr and a substrate temperature of 710–760 °C. The $SrTiO_3$ film grows in two different orientations separated by a 45° grain boundary. In the growth plane the epitaxial relations are $SrTiO_3[110]//Al_2O_3[11\bar{2}0]$ and $SrTiO_3[100]//MgO[100]//Al_2O_3[11\bar{2}0]$, as illustrated in

 0003-6951/91/310733-03$02.00

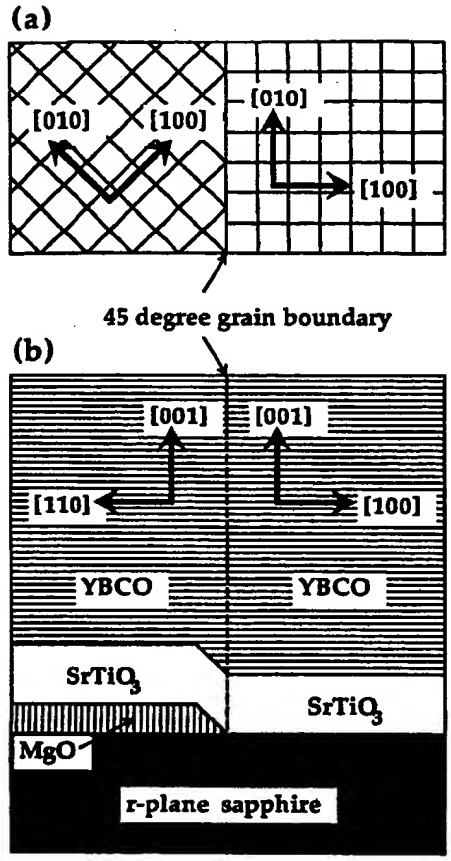

FIG. 1. Schematic view of the device structure with an MgO seed layer and a $SrTiO_3$ buffer layer on an *r*-plane sapphire substrate. (a) top view, (b) side view.

Fig. 1. We then immediately deposit YBCO, which grows epitaxially everywhere and thereby reproduces the grain boundary in the $SrTiO_3$ buffer layer. Finally the YBCO is patterned into an appropriate geometry.

The virtue of this structure is that, apart from the predefined 45° grain boundaries, there are no other high-angle grain boundaries in the YBCO film. It has been reported[12] that YBCO films grown on $SrTiO_3$ buffer layers on *r*-plane sapphire substrates have high critical current density and low surface resistance. In addition, the $SrTiO_3$ layer grown on the MgO buffer layer does not have any high-angle grain boundaries, as demonstrated in a ϕ scan of the $SrTiO_3$ (101), although it is found[13] that YBCO deposited on MgO may have a number of high-angle grain boundaries. The probable explanation for this effect is that the energy needed to nucleate 45° misoriented $SrTiO_3$ grains on MgO is much higher than in the case of YBCO grown on MgO. Hence the YBCO film on $SrTiO_3$ on MgO also lacks any high-angle grain boundaries and has a high critical current density. Microbridges formed either side of the predetermined grain boundary have critical current densities of $1-3\times10^6$ A/cm^2 at 77 K. In order to show that the critical current reduction is indeed due to the grain boundary rather than simply the step at the edge, we etched only part of the MgO, reducing its thickness on one side from 20 to 10 nm, such that YBCO/$SrTiO_3$/MgO

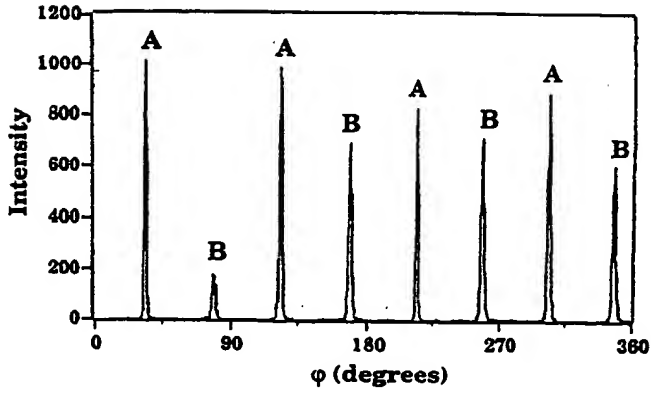

FIG. 2. X-ray ϕ scan of YBCO (103) of the unpatterned structure. The peaks labeled with "A" belong to YBCO/$SrTiO_3$/Al_2O_3 and the peaks labeled with "B" come from YBCO/$SrTiO_3$/MgO/Al_2O_3.

remained on the sapphire substrate on both sides of the step.The critical density across this step remained larger than 10^6 A/cm^2 at 77 K.

A ϕ scan of the YBCO (103) before the last patterning process is shown in Fig. 2. The peaks occurring 45° apart indicate that half of the YBCO is rotated 45° relative to the other half. Suitable etching experiments have shown that the peaks labeled with "A" belong to YBCO/$SrTiO_3$/Al_2O_3 and the peaks labeled with "B" come from YBCO/$SrTiO_3$/MgO/Al_2O_3. Cross-sectional transmission electron microscope images and microdiffraction patterns show that the 45° grain boundary begins at the end of the MgO seed layer.[14]

As the first example of a device using multiple junctions made with our process we fabricated a square washer SQUID[15] as shown in the inset of Fig. 3. It was patterned across the grain boundary by photolithography and wet etched with dilute phosphoric acid. The current-voltage characteristic (*I-VC*) of the SQUID at 4.2 K, which ex-

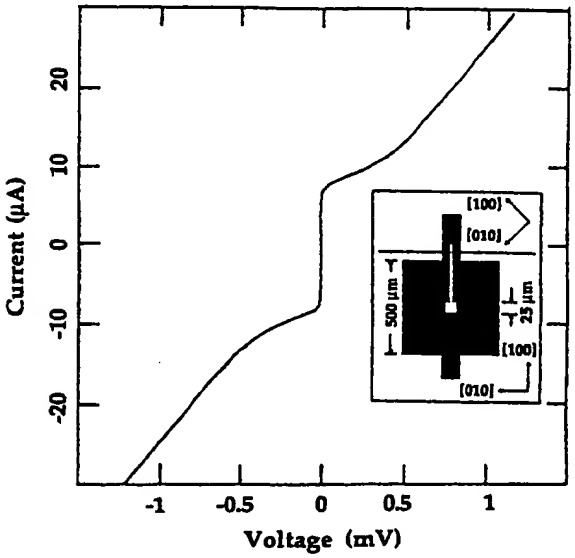

FIG. 3. Current (vertical)-voltage (horizontal) characteristics of a dc SQUID at 4.2 K. The inset shows the geometry of the SQUID.

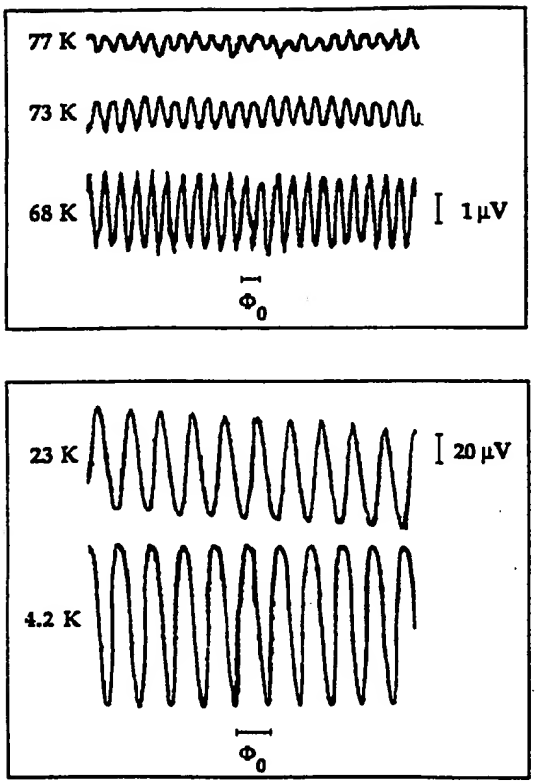

FIG. 4. Modulation voltage of the current-biased dc SQUID vs applied magnetic flux at various temperatures.

hibits resistively shunted Josephson junction behavior, is shown in Fig. 3. Each junction was 4 μm wide and 0.2 μm thick. The critical current of about 10 μA at 4.2 K translates to about 10^3 A/cm^2 critical current density across the junctions. The I_cR_n product of the junctions is about 420 μV at 4.2 K. The *I-VC* of the SQUID at 77 K shows no zero resistance part, although it is nonlinear. The small junction coupling energy $I_c\Phi_0/2\pi$ compared to the thermal energy k_BT may lead to thermally activated phase slippage across the junctions, resulting in resistance at all currents.[16] Detailed transport properties of the junctions including the magnetic field dependence of the critical current will be reported elsewhere.[17]

The voltage across the current-biased dc SQUID as a function of applied field is shown for various temperatures in Fig. 4. The data were taken in a bandwidth of 0–10 Hz without any signal averaging. The observed period corresponds to the expected value from the geometry of the SQUID. We believe that the reduction of the modulation voltage at high temperatures is due to the decreasing critical current and the large inductance of the SQUID. We have observed dc SQUID operation at temperatures as high as 88 K and have operated such a SQUID in a flux-locked loop up to 83 K. The noise of this SQUID is similar to that reported in dc SQUIDs made using bicrystal substrates.[10] Detailed performance of the SQUID will be published elsewhere.[18]

A further example of small-scale integration using biepitaxial grain boundary junctions is provided by a flux shuttle[19] we have fabricated. It involves two dc SQUIDs as sensors and eleven more bi-epitaxial junctions as switching elements. Our work on such integrated circuits is continuing and will be reported later.

In summary, we have reported the development of bi-epitaxial grain boundary junctions in $YBa_2Cu_3O_7$ at multiple and predetermined locations by using only standard photolithographic techniques to control in-plane epitaxy with seed and buffer layers. The junctions have current-voltage characteristics that are well described by the resistively shunted junction model and dc SQUIDs fabricated using these junctions show modulation at temperatures as high as 88 K. By increasing the critical current density of the junctions and lowering the inductance of the SQUID, the performance of the SQUIDs should improve further, especially at 77 K. We believe that this technology, based on bi-epitaxial grain boundaries, can be extended to integrated circuits in the near further, and we are planning to demonstrate such circuits.

We would like to thank John Rowell, Mac Beasley, Ted Geballe, Bob Hammond, John Clarke, Aharon Kapitulnik, Randy Simon, and Roger Barton for helpful discussions on this work. We also would like to thank Jeff Rosner at Hewlett–Packard for the TEM studies.

[1] D. Dimos, P. Chaudhari, J. Mannhart, and F. K. LeGoues, Phys. Rev. Lett. 60, 1653 (1988).
[2] R. H. Koch, W. J. Gallagher, B. Bumble, and W. Y. Lee, Appl. Phys. Lett. 54, 951 (1989).
[3] S. E. Russek, D. K. Lathrop, B. H. Moeckly, R. A. Buhrman, D. H. Shin, and J. Silcox, Appl. Phys. Lett. 57, 1155 (1990).
[4] R. B. Laibowitz, R. H. Koch, A. Gupta, G. Koren, W. J. Gallagher, V. Foglietti, B. Oh, and J. M. Viggiano, Appl. Phys. Lett. 56, 686 (1990).
[5] K. P. Daly, W. D. Dozier, J. F. Burch, S. B. Coons, R. Hu, C. E. Platt, and R. W. Simon, Appl. Phys. Lett. 58, 543 (1991).
[6] D. B. Schwartz, P. M. Mankiewich, R. E. Howard, L. D. Jackel, B. L. Straughn, E. G. Burkhart, and A. H. Dayem, IEEE Trans. Magn. 25, 1298 (1989).
[7] C. T. Rogers, M. S. Hedge, B. Dutta, X. D. Wu, and T. Venkatesan, Appl. Phys. Lett. 55, 2032 (1989).
[8] J. Gao, W. A. M. Aarnink, G. J. Gerritsma, G. Veldhuis, and H. Rogalla, IEEE Trans. Magn. 27, 3062 (1991).
[9] D. K. Chin and T. Van Duzer, Appl. Phys. Lett. 58, 753 (1991).
[10] R. Gross, P. Chaudhari, M. Kawasaki, M. B. Ketchen, and A. Gupta, Appl. Phys. Lett. 57, 727 (1990); Physica C 170, 315 (1990).
[11] S. M. Garrison, N. Newman, B. F. Cole, K. Char, and R. W. Barton, Appl. Phys. Lett. 58, 2168 (1991).
[12] K. Char, N. Newman, S. M. Garrison, R. W. Barton, R. C. Taber, S. S. Laderman, and R. D. Jacowitz, Appl. Phys. Lett. 57, 409 (1990); K. Char, N. Newman, S. M. Garrison, R. W. Barton, G. Zaharchuk, S. S. Laderman, R. C. Taber, and R. D. Jacowitz, presented at Applied Superconductivity Conference, Aspen, Colorado (1990).
[13] S. S. Laderman, R. C. Taber, R. D. Jacowitz, J. L. Moll, C. B. Eom, T. L. Hylton, A. F. Marshall, T. H. Geballe, and M. R. Beasley, Phys. Rev. B 43, 2922 (1991).
[14] S. J. Rosner (private communication).
[15] M. B. Ketchen and J. M. Jaycox, Appl. Phys. Lett. 40, 736 (1982).
[16] R. Gross, P. Chaudhari, D. Dimos, A. Gupta, and G. Koren, Phys. Rev. Lett. 64, 228 (1990).
[17] P. Rosenthal, A. Barrera, M. R. Beasley, K. Char, M. S. Colclough, and G. Zaharchuk (unpublished).
[18] M. S. Colclough, K. Char, G. Zaharchuk, A. H. Miklich, and J. Clarke (unpublished).
[19] T. A. Fulton, R. C. Dynes, and P. W. Anderson, Proc. IEEE 61, 28 (1973).